MXene-based ternary composites for supercapacitors: Advancements and challenges

Kabir O. Otun [a b], Azfarizal Mukhtar [a], Ismail Hossain [c], Jibril Abdulsalam [d]

[a]Institute of Sustainable Energy, Putrajaya Campus, Universiti Tenaga Nasional, Jalan IKRAM-UNITEN, 43000 Kajang, Malaysia
[b]Department of Physics, University of Pretoria, 0002 Pretoria, South Africa
[c]Department of Nuclear and Renewable Energy, Ural Federal University, Yekaterinburg 620002, Russia
[d]Institute of Materials Science, Technical Institute of Darmstadt, 64287 Darmstadt, Germany

*Corresponding author at: Institute of Sustainable Energy, Putrajaya Campus, Universiti Tenaga Nasional, Jalan IKRAM-UNITEN, 43000 Kajang, Malaysia. Email: otun.kabir@uniten.edu.my

Highlights

- MXene ternary composites produce synergistic effects that enhanced supercapacitor performance.
- MXene ternary composites with metal oxides possess good electrical conductivity and rich redox activity.
- MXene ternary composites also show promising results in micro-supercapacitors.
- This work helps to optimize MXene ternary composites for energy storage devices.

Abstract

The acceleration of the global energy transition and the achievement of Sustainable Development Goals (SDGs) depend on promoting innovation in energy storage technologies. MXenes and their composites have emerged as novel electrodes for electrochemical energy storage. Numerous investigations into MXene binary nanocomposites have shown that they can deliver enhanced electrochemical performance when compared to their pristine forms. However, strong van der Waals forces between layers in MXene nanosheets can result in restacking, which lowers capacitance and slows kinetics, thereby limiting their practical applications. To achieve an enhanced electrochemical performance, attention has been shifted to MXene-based ternary nanocomposites for supercapacitors. In comparison to the previous binary system, these unique ternary MXenes display newly produced features and high-performance activity. This promotes synergism and results in superior capacitance, charge transfer kinetics, high specific energy and power, and enhanced stability. Nevertheless, based on the review of the literature, not much work has been done to prepare and investigate this novel ternary nanostructure for supercapacitors. Therefore, this review provides insights into recent advances in MXene-based ternary composites with a view to establishing the connection between their properties and supercapacitor performance. The performance of MXene-based ternary composites in supercapacitors and micro-supercapacitors are enumerated, including their practical applications. Finally, challenges and outlooks for further improving the performance of ternary composites in energy storage are highlighted.

Keywords: MXene; Supercapacitors; Ternary composite; SDGs; Energy transition

1. Introduction

The fast expansion of energy consumption and industrialization have made it compelling to harness renewable resources including solar, thermal, wand wind for sustainable energy conversion and storage [1]. However, since renewable supplies are erratic, integrating energy storage units with innovative electronics is a crucial first step toward a steady power supply [2]. The most popular energy storage devices are supercapacitors and batteries because of their exceptional efficiency and environmental friendliness [3]. The two energy devices can help harvest energy from renewable sources and deliver continuous power. Batteries are characterized by high specific energy, and their working principle is based on ion intercalation [4]. However, owing to their low power density and short lifespan, they require regular replacement and maintenance. Additionally, batteries cannot be used in some applications where a significant current spike is required because of their poor power density. On the other hand, supercapacitors (SCs) store charges through the adsorption of electrolyte ions onto the surface of electrode materials or pseudocapacitive faradaic interactions (between the surface of the electrode material and the ions in the electrolyte). On the other hand, supercapacitors store charges through the adsorption of electrolyte ions onto the surface of electrode materials or pseudocapacitive faradaic interactions (between the surface of the electrode material and the ions in the electrolyte) [5]. While SCs have a lower energy density than batteries, they can operate a variety of electronics for several hours. Hence, supercapacitors are better options than batteries in terms of power density and cycling stability [6]. Based on charge storage mechanism, supercapacitors are grouped into two; the electric double layer capacitors (EDLC) with rapid physical adsorption/desorption and pseudocapacitors based on reversible redox reactions. Carbon-based materials constitute the EDLC, while conductive polymers and metal oxides/sulfides are examples of electrode materials used for pseudocapacitors [7,8].

The intriguing characteristics of two-dimensional nanomaterials, including as their enormous specific surface areas, atomically thin 2D nature, mechanical flexibility, and physical and chemical properties, have also linked them to possible electrode materials for SCs [9]. MXenes, or transition metal carbides, nitrides, and carbonitrides, belong to the 2D material family and have attracted a lot of interest in SCs because to their remarkable hydrophilic qualities, mechanical stability, and conductivity [10]. The name MXene was coined from graphene because they have some characteristics. The MAX phase, which is the precursor of mXene, has the chemical formula $M_{n+1}AX_n$ (n = 1 to 4). A is an element of groups 13–15 of the periodic table (Al, Ga, In, Si, Ge, As, Sn, Pb, etc.), X is carbon and/or nitrogen, and M is an early transition metal (Ti, V, Cr, Mn, Zr, Nb, Mo, Ta, etc.) [10,11]. The periodic table is used to show the various elements of MAX phases in Fig. 1. MXenes are produced by etching their parent MAX phases selectively, such as $Ti_3C_2T_x$ (T_x = — F, — O, and/or — OH) from Ti_3AlC_2. MXene-based supercapacitor electrodes exhibit remarkable pseudocapacitive behavior, with a theoretical specific capacitance of up to 1116 F g^{-1}. This is attributed to their redox-active surface that resembles metal oxide and their intrinsic metallic conductivity of up to 20,000 S·cm^{-1} [12]. Numerous studies were able to produce extremely flexible free-standing films by taking advantage of their nanoscale mechanical flexibility [13,14]. These films demonstrated their adaptability in supercapacitor applications by easily functioning as supercapacitor electrodes via direct vacuum filtration of MXene dispersions [15]. MXene also provides a great degree of physicochemical tunability. This is accomplished by altering the synthesis method, the choice of precursors, and kinetically regulating the synthesis procedures. Thus, to enable high-rate, high-volume electrochemical energy storage of MXene-based supercapacitors, it is advantageous to readily alter MXene attributes including electrical conductivity, nanosheet flake sizes, and surface termination components [16,17].

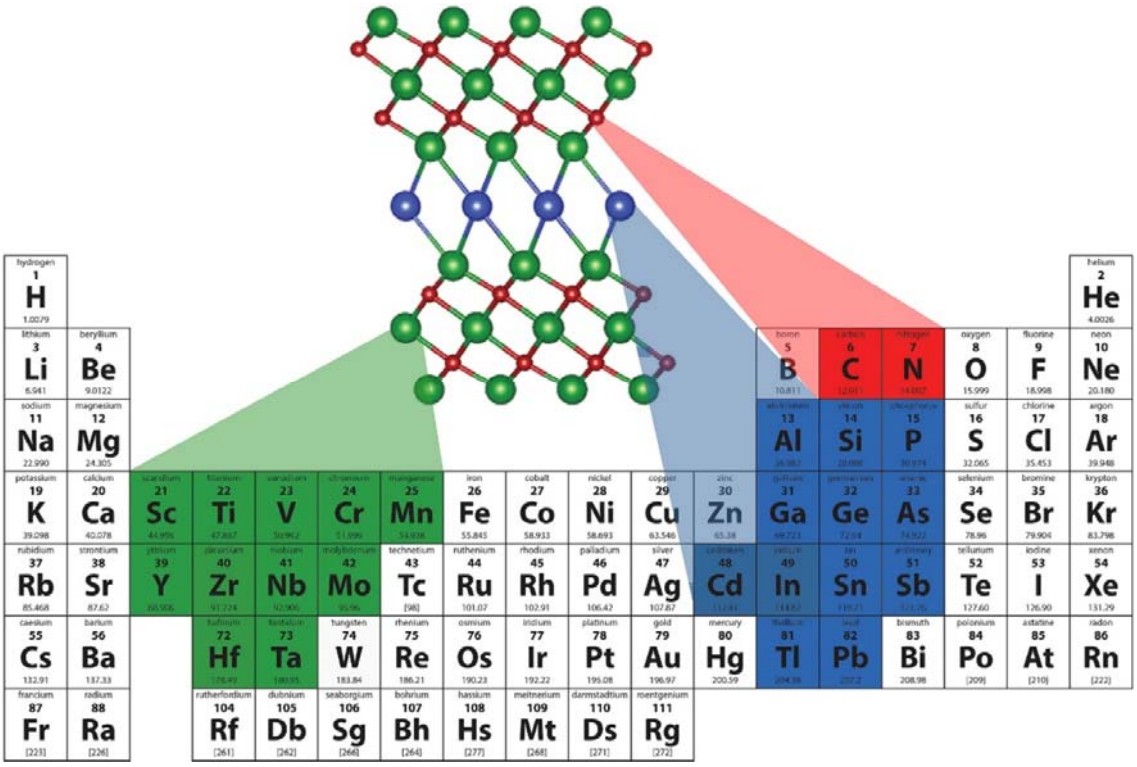

Fig. 1. Periodic table illustrating the elements of MAX phases. Reproduced with permission from [18] Copyright 2019, Elsevier.

Despite the good electrochemical properties of MXenes, there are still issues that need to be resolved, including low capacitance, low energy density, and layer restacking [19]. A variety of techniques, including doping, surface modification, morphological control, and hybrid composites incorporating conducting polymers, carbonaceous materials, and transition metal oxides (TMOs), have been employed to overcome these issues and improve the performance of MXene-based electrodes in SCs [15]. To utilize more of its fascinating qualities, MXene is tailored to fabricate an open material architecture and is easy to combine with other materials to construct binary composites and ternary composites [20]. Recently, ternary MXene composites have garnered great interest as some binary composites cannot match the requirements of the high-performance supercapacitor. As a result, numerous strategies have been put in place to fabricate MXene ternary composites for high-performance supercapacitor applications by combining three distinct types of electroactive materials [21]. Unfortunately, there are currently no thorough review on the ternary MXene composites for supercapacitors. Therefore, this review provides a thorough overview of the research progress and opportunities of ternary MXene composites in supercapacitors. It specifically covers the structural architecture and reasoning behind investigating various composites, their electrochemical performances, and limitations for further studies. First, we gave a brief overview of supercapacitor technology and explained the charge storage process of MXenes in supercapacitors. This is followed by highlights of various factors influencing the performance of MXenes in supercapacitors. To explain the recent development of ternary MXene composites and their potential to concurrently attain high specific capacitance and rate performance, the binary MXene composites and their limitations in supercapacitors are introduced. The applications of ternary MXene composites in supercapacitors and micro

supercapacitors are explained. Finally, the obstacles, and prospects of using ternary MXene composites to push the boundaries of MXene-based supercapacitors are summarized (Fig. 2).

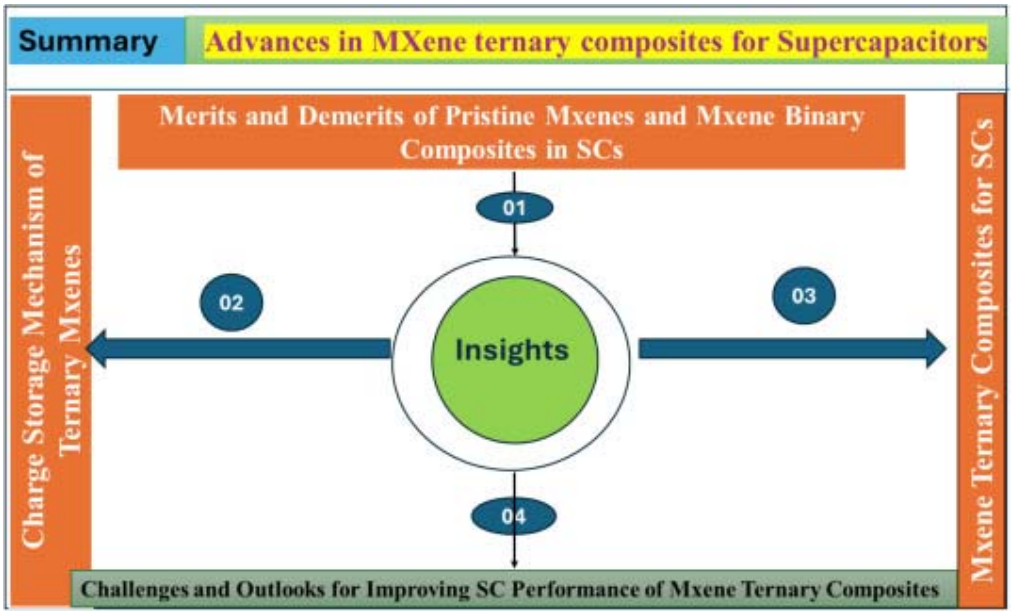

Fig. 2. Scheme illustrates the scope of the review on the insights of MXene ternary composites for supercapacitors.

2. Key information on supercapacitor technology

Supercapacitor technology is a rapidly advancing field that offers unique advantages for various applications [22]. They store electrical energy in an electric double-layer formed at the interface of electrolyte and high-surface-area electrodes. This mechanism allows for the rapid storage and release of energy without the need for chemical reactions, making them distinct from traditional batteries. Supercapacitors are typically characterized by their high-power density, allowing them to deliver quick bursts of energy. However, their energy density is lower than that of batteries (Fig. 3). Researchers continue to work on improving energy density to expand the range of applications [23]. These offer a practical way to supply energy in remote locations without access to public grids or where the expense of connecting and supplying electricity is high. SCs can also be utilized as power sources for portable electronics such as laptops, digital cameras, mobile phones, and so on because they are small, light, and flexible. In addition to shielding the batteries from high frequency rapid charging and discharging (dynamic operation) and preserving energy, SCs can be utilized in electric and hybrid vehicles to offer the high-power density required for rapid acceleration and energy recovery during braking [24]. The Ragone plot is used to depict the power density (P_d) and energy density (E_d). This diagram shows that SCs are high-power systems than batteries and possess the ability to provide intermediate power and energy. Other benefits of SCs include safety and environmental friendliness because, unlike rechargeable batteries, these devices do not require vast amounts of electrolytes, making them incredibly safe to use and simple to recycle.

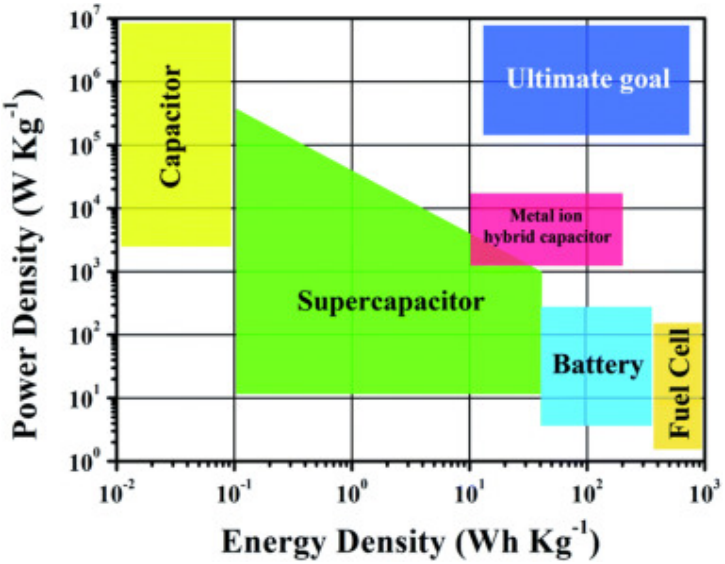

Fig. 3. Ragone plot of several electrochemical energy devices. Reproduced with Permissions from [25]. Copyright 2020, Royal Society of Chemistry.

Supercapacitors are classified into two according to their storage mechanism: 1), electrostatic double-layer capacitors (EDLCs) which rely on the double-layer capacitance at the electrode-electrolyte interface and are suitable for applications that require high power output and fast charge/discharge cycles, and 2) pseudocapacitors that involve Faradaic redox reactions at the electrode material, offer a higher energy density but slightly slower charge and discharge rates [26]. Pseudocapacitors are often used when a balance between energy and power is required. Supercapacitor technology represents a promising solution for energy storage and delivery in a wide range of applications [27]. As advancements continue to drive improvements in energy density and cost-effectiveness, supercapacitors are likely to become increasingly vital in addressing the world's energy needs, particularly in high-power, quick-response applications [28]. The primary problem with supercapacitors is still their low energy density value, however because of the close correlation between their squared capacitance (Ed) and voltage (V), increasing one or both of these variables will result in a higher energy density. Further aid in delivering increased energy density may be provided by utilizing electrode materials with high specific capacitance, electrolytes with broad potential windows, and integrated system structure optimization [28].

The two and three electrode configurations are distinctive architectures of a supercapacitor [29]. Three electrode cells are mostly utilized for obtaining measurements during research studies due to their higher level of accuracy, whereas two electrode cells are employed in both research studies and broader commercial applications [30]. A three-electrode layout adds a reference electrode to enhance measurement precision, while a two-electrode cell comprises two electrodes, metallic current collectors, and separators [31].

3. Specialty of MXenes as electrode materials for supercapacitors

The adaptability of MXenes has fascinated materials experts even though they were just discovered a dozen years ago [32]. These conductive 2D layered nanomaterials have a higher energy storage capacity than materials used in batteries and supercapacitors, and are incredibly strong, and impenetrable to electromagnetic radiation. MXenes, a relatively recent class of two-

dimensional materials, have gained significant attention in the field of supercapacitor technology due to their unique properties that make them excellent electrode materials [32]. These features include, but not limited to exceptional mechanical strength, high conductivity and stability—that is, they can be arranged in 3D architectures with enough nanomaterial volume and large surfaces available for reactions [33]. Specifically, $Ti_3C_2T_x$ MXenes exhibit a large capacitance due to their abundance of redox sites. The hydrogenation of the oxygen-containing terminal group causes “Ti” to fluctuate in its oxidation state. On the other hand, there is almost a linear relationship between the potential change and the “Ti” oxidation state change [34]. The dimensions of the electrolyte cations, surface terminations, morphology, interlayer spacing, and other factors all affect the capacitance characteristics of $Ti_3C_2T_x$ [33]. When electrolytic cations intercalate between the $Ti_3C_2T_x$ interlayers, an electrostatic attraction between opposing charges is generated. Consequently, the cations will intercalate through the interlayers if their size is smaller than the interlayer gap. Pseudocapacitive behavior will arise from this rapid redox reaction. Excellent cycle stability is maintained, however, because large cations are unable to pass through the interlayers and generate electrostatic repulsion at the interlayer edge. The cations' surface adsorption will consequently give rise to the electric double-layer capacitance [35]. The electrochemical behavior and performance of MXenes may be significantly impacted by varying techniques that result in distinct MXene structures and surface chemical states. Furthermore, MXenes exhibit exceptional mechanical flexibility, good dispersibility in a range of solvents, and tunable porosity [36]. MXene aqueous solutions exhibit a strong Tyndall effect and are particularly stable because of the hydrophilicity and electrostatic repulsion between lamellar components. A variety of techniques, including vacuum filtration, coating, and printing, can be used to quickly produce flexible MXene films. Spinning can also be used to make bendable MXene fibers. Structural integrity is maintained in most cases, and flexible storage devices are built with good mechanical performance. Under various deformation situations, reliable electrochemical performance is ensured by excellent flexibility [37].

Compared to traditional carbonaceous materials, the remarkable properties of MXenes such as its huge density electric conductivity, hydrophilic nature, and very faradic pseudocapacitive nature have shown that they can be used as an ultra-high volumetric capacity supercapacitor [38]. Thus, MXenes could be used as current collectors for electron transport and as active materials for charge storage. Due to these properties, extra dense Cu current collectors won't be needed, and MXene supercapacitors with large area and volumetric capacities can be developed, moving the field of smart electronics forward. Symmetric SCs (SSCs) and asymmetric SCs (ASCs) are the two main categories of MXene-based SCs. It is still difficult to find a positive electrode for ASCs with the same conductivity and rate performance as the negative MXene electrode, despite the fact that the potentials of both electrodes can be used to control the cell voltage. The electrode kinetics and charge storage capacities vary due to the non-uniform value that results from fully utilizing charge-storage capacities at varying charge/discharge rates.

3.1. Charge storage mechanism of MXenes in supercapacitors

There are different charge storage techniques used in the field of electrochemistry. For EDLC to function optimally, a double layer must form at the electrode-electrolyte interface [39]. This phenomenon is most commonly seen in carbon-based electrodes like graphene and carbon fibers. The surface area of the electrode material has a direct correlation with the performance of EDLCs. Their energy density is, however, limited by the trade-off between specific surface area and capacitance performance. Pseudocapacitors are a type of electrochemical capacitor in

which charge is held at the electrode surface by fast Faradaic reactions using conducting polymers and transition metal oxides. In this case, the electrode's surface redox centres are essential for pseudocapacitive energy storage. Pseudocapacitors have better energy density than capacitors, but their rate performance is frequently inferior [39].

MXene's charge storage mechanism is not unitary. Rather, it is affected by surface terminations, the kind of electrolyte ions, and the strength of the electrostatic potential difference imposed across the electrode/electrolyte interface [40]. MXene is most likely to represent EDLC capacitance in an H^+-deficient environment, like in neutral (KNO_3, and $MgSO_4$) and basic electrolytes, while when using acidic electrolyte, it is primarily supported by pseudocapacitive behaviors. The process of ion intercalation in an aqueous solution, in the case of pseudocapacitors, allows charge storage using MXene layers. Different ions occupy electrochemically active sites on the MXene surface and reversibly intercalate the MXene layers, contributing to the energy storage mechanism [40]. For instance, the electrochemical performance of $Ti_3C_2T_x$ MXene in an ionic liquid electrolyte was investigated by Lin et al. Broad peaks were visible on the cyclic voltammograms at −0.2 and 0.6 V. Pseudocapacitance features in aqueous systems are not expected to result from —O and —F terminations in $Ti_3C_2T_x$ MXene, as these terminations prevent MXene from becoming electrochemically active in the electrolyte of ionic liquids [41].

The interactions and intrinsic features of ions, such as their electronegativity, surface energy, interaction energy, ionic radii, and valence states, have a significant impact on the electrochemical performance of the composites of MXene-based SCs. The intercalated ions provide incremental charge or neutral size throughout the charge storage process, which leads to the quick electron delocalization of doped MXenes through strong ionic interactions, hydrogen bonds, and electrostatic adsorption. The interactions between the doped MXene and the stored ions differ, depending on the surface M layers and outermost TX layers, which can either encourage or inhibit ion shuttling. If a significant number of ions may intercalate, a high-capacity doped-MXene-based electrode can be constructed, but the rate capability may be compromised [42].

4. Modifications of MXenes for supercapacitors

MXenes are a promising electrode for energy storage applications due to several unique properties, including their high young modulus, exceptional thermal and electric conductivities, tuneable band gap, and availability of electrochemically active sites. MXenes can provide significant capacitance and a reasonable cycle life when utilized as supercapacitor electrodes [41]. However, pure MXenes are generally hindered by diminishing mechanical strength and restacking. As such, it is preferred to build an MXene heterostructure with other materials to overcome problems of MXene as an electrode in supercapacitors. The following modifications are necessary to achieve this:

4.1. Surface functionalization

Surface functionalization of MXene like heteroatom doping can alter its electrochemical performance in supercapacitors [43]. Numerous studies have investigated the nexus between the N-atom and MXene electrochemistry and found that the N-atom is an active heteroatom. Freshly synthesized MXenes have functional groups on their surfaces called —O, —F, and —OH, which always raise the possibility of oxidation or interaction with other materials [44]. The functional groups on the MXene surfaces, especially around the edges where oxidation

happens quickly, create a channel for the MXene sheets to degrade once they are exposed to air [45]. For example, a Ti_3C_2 film with a flexible N-doping layer was produced by static adsorption and in situ solvent heat treatment, where an alcohol solution saturated with urea was used as a source of N-atoms. Moreover, N intercalation increased the layer spacing in MXene, indicating that it offers a technique of modifying the electrochemical properties [46]. Alkali etching is a technique that can be used to generate Mxenes without —F functional groups. The multilayer $Ti_3C_2T_x$ obtained via HF treatment has a lower gravimetric capacitance than the $Ti_3C_2T_x$ prepared by the alkali-assisted hydro-thermal technique in NaOH aqueous solution, without the —F terminations [47].

4.2. Size and morphology of MXene

The sheet size influences the supercapacitor performance of MXenes generated during the etching method [48]. It has been established that MXene with large sheet sizes is appropriate for supercapacitors; nevertheless, the prolonged etching time of these huge sheets is one of the main issues [49]. By offering more metallic and electrochemical active sites over the surface during the charging-discharging process, smaller MXene sheets can improve supercapacitor performance. Using, for example, the same amount of highly conductive large-size Ti3C2Tx flakes and ion-channel-rich small-size $Ti_3C_2T_x$ flakes, Kayali et al. created free-standing electrodes with high specific and volumetric capacitance values of about 435 F g^{-1} and 1513 F cm^{-3}, respectively [50]. The size of the two-dimensional flake is shown to have a considerable effect on the electrochemical performance of the $Ti_3C_2T_x$ electrode, which was enhanced by regulating the flake size. As a result, regulating the flake size is key to modifying the performance of the electrode. The electrochemical performance of MXene-based supercapacitors can be improved by a 3D porous structure with a large surface area because it allows for complete contact with electrolyte ions and shortens the transport path [51]. These $Ti_3C_2T_x$ sheets was then assembled by wet spinning into flexible macroscopic ribbons or fibers. The highly oriented and cross-linked structure present in the interfacial area gives $Ti_3C_2T_x$ superior mechanical properties and exceptional conductivity. This leads to a volumetric capacitance of 1570.5 F·cm^{-3} and 99.5 % capacitance retention even in the knotted state for wearable devices [52].

The morphology of MXene is another significant factor that influences its supercapacitor performance which may further be tuned by the synthesis protocol. To enhance the ion transport rate to active redox sites and augment the electrochemically accessible surface area of MXenes [50], it is imperative to design an open structure and customize the morphology of MXene nanosheets. To get high capacitance and power performance, several tactics have been put forth, including regulating flake size, increasing interlayer spacing, creating three-dimensional (3D) porous structures, vertical alignments, etc. For instance, the study conducted by Sugahara et al. employed the 2D material $Ti_2C_2T_2$ to investigate the impact of confinement effect on capacitance performance which enhanced supercapacitor performance [53].

4.3. Synthesis method

The pseudocapacitive behavior in MXenes is produced via a bulk redox process involving rapid ion intercalation [54]. Consequently, greater ion intercalation and electrolyte exposure may result from an increase in the interlayer gap, both of which may contribute to an increase in energy density. When MXene is delaminated by sonication or intercalation with cations or big molecules, the interlayer gap is increased, which raises the capacitance. According to Yang et al. [55], ex-situ N-doping using solvothermal method allows for control over the nitrogen

content, while in situ N solid solution doping (TN-Ti_3C_2) does not allow for this control. Because of this characteristic, ex-situ N-doped MXenes with increased capacitance are more dependable. At a scan rate of 5 mV cm^{-3} in a 3 M H_2SO_4 electrolyte, the N-doped Ti_2CT_x MXenes produced by urea (UN-Ti_3C_2) and monoethanolamine (MN-Ti_3C_2) assisted solvothermal technique demonstrated a good volumetric capacitance of 2836 F cm^{-3} and 2643 F cm^{-3}, respectively. After 20,000 cycles, the UN-Ti_3C_2 and MN-Ti3C_2 films showed capacitance retention of around 81.7 % and 100 %, respectively. The UN-Ti_3C_2 film was used to produce a symmetric device with an exceptional specific energy of 76 Wh/L, indicating that this approach is very appropriate for producing supercapacitors [55].

Recently, molten-salt-assisted strategy has been established as a promising route to prepare 2D MXenes with high conductivity, remarkable mechanical strength, and rich surface chemistries to match the requirement for real-world applications [56]. Through molten salt thermal treatment, Xu et al. prepared N-doped $Ti_3C_2T_x$ using LiCl-KCl salt as the solvent and Li_3N as the nitrogen supply. The delamination of $Ti_3C_2T_x$ multi-layers into a few layers was caused by increasing the d-spacing of the $Ti_3C_2T_x$ layers by optimizing the mass ratio of Li_3N: $Ti_3C_2T_x$ to 1:2. Furthermore, there was a significant decrease in the F element and a significant increase in the N content in $Ti_3C_2T_x$. As a result, due to its high electrochemical activity area and good electrical conductivity, the N-doped N-$Ti_3C_2T_x$-0.5 electrode demonstrated excellent capacitance retention (87.5 % after 10,000 charging-discharging cycles), good rate performance (83.1 % at 20 A g^{-1}), and a higher specific capacitance (332 F g^{-1} at 0.5 A g^{-1} in 1 M H_2SO_4 solution) [57].

4.4. Electrode design

The adjustment of the electrode architecture is also key to the performance of MXenes [58]. Micro-supercapacitors with a planar electrode structure are ideal for suitable integration of microelectronic systems [59]. Ion diffusion is facilitated by this planar arrangement over sandwich equivalents. $Ti_3C_2T_x$ based on-chip MSCs were prepared by using a coating, processing, and cutting process to hydrophilic Si/SiO_2 chips to deposit $Ti_3C_2T_x$ at a thickness of around 600 nm [51]. The enhanced uniformity and integrity of MXene film demonstrated a high capacitance of 4.72 F·cm^{-2} (21.4 F·cm^{-3}) and 87.6 % capacitance retention after 10,000 cycles without the need for current collectors. Likewise, the hydrogel $Ti_3C_2T_x$ MXene electrodes showed remarkable volumetric capacitance reaching over 1500 F cm^{-3}. Macroporous MXene electrode designs with an open structure, enabled by a polymethyl methacrylate microsphere or a MgO nanoparticle template-based approach, exhibit excellent rate performance. Moreover, the $Ti_3C_2T_x$ flakes can be vertically aligned by mechanically shearing a discotic lamellar liquid-crystal phase of $Ti_3C_2T_x$ MXene [60]. The resulting electrode films exhibit nearly independent electrochemical performance from film thickness (around 200 nm). The 3D $Ti_3C_2T_x$ aerogel was created using an EDA-assisted self-assembly approach. It has a specific surface area of 176.3 m^2g^{-1} and a 3D network structure with large mesopores and micropores. An outstanding result of 1012.5 mF cm^{-2} in 1 M KOH electrolyte was observed. Because of its improved mechanical properties and the absence of pseudocapacitive processes in the electrode reaction, the electrode maintains 84 % of its initial specific capacitance after 5000 cycles [60].

4.5. Electrolyte

The performance of a supercapacitor electrode is dependent on the nature of electrolyte, and MXene is no exception [61]. There are basically four types of electrolytes: solid, ionic, organic,

and aqueous. The electrolytes are accountable for the supercapacitor's potential window during measurements. The larger pseudocapacitive nature of MXene-based materials in acidic conditions enables larger volumetric capacitance [62]. Additionally, the material displays EDLC behavior when used with sulfide-based electrolytes such as Na_2SO_4 or K_2SO_4. The volumetric capacitance of MXene can be as high as 1500 $F \cdot cm^{-3}$ when combined with an H_2SO_4 electrolyte hydrogel. However, conventional electrolytes are limited in applications for use in device fabrication. Instead, gel electrolytes, such as PVA/Na_2SO_4, are commonly used, but they also have issues with suppression of the voltage window and an overall reduction in electrochemical performance. For this reason, other electrolytes like organic and ionic liquid-based electrolytes are employed. MXene-based supercapacitors have profited from the explosion of research on novel electrolytes, such as water-in-salt or ionic liquids [63]. These devices have demonstrated an approximately 1.2 V potential window expansion, and thereby increasing their energy density. For instance, a wide voltage window of 3 V was obtained in $Ti_3C_2T_x$ based supercapacitors by applying 1-ethly-3-methylimidazolium bis-(trifluoromethylsulfonyl)-imide in CH_3CN as the electrolyte. The electrode delivered a capacitance of 70 F g^{-1} at a s can rate 20 mV s^{-1}, owing to the large interflake spacing of the MXene as well as the disordered structure [64].

5. Advancement in MXene-based electrode for supercapacitors

The remarkable properties of MXenes including electrical conductivity, and flexibility make them ideal for the fabrication of various supercapacitor devices, including micro-supercapacitors and solid-state supercapacitors. Additionally, many 2D MXene cations can participate in energy storage by reversibly intercalating into nanomaterials and occupying redox-active sites. Before being intercalated into layers, ions usually become adsorbed on the exterior surface or the edges of 2D MXene NMs. High rate capability, advantageous cycle stability, pseudocapacitive behavior, and ultrahigh volumetric capacitance are all provided by pure MXenes and MXene-based composites. Combinations of different functional qualities are made possible by the assembly of hybrid materials, which are not possible with pristine materials. Conducting polymers (CPs), metal compounds, and carbonaceous materials have all been combined with MXenes to create a variety of MXene-based composites. As a result, a synergistic effect was achieved, whereby MXenes' exceptional electronic conductivity contributed to the quick movement of electrons, increased surface area that was available, and stabilized the structure of the materials. Additionally, by acting as a spacer and enlarging the interlayer distance, these materials stop the MXene nanosheets from restacking. As a result, ions are more readily accessible and move through space more quickly. As a result, MXene-based nanocomposites have outperformed active materials and pure MXene in terms of electrochemical performance.

5.1. MXene binary composites for supercapacitors

MXene binary composites are a class of materials that combine MXenes with another component, such as a conductive material or a metal oxide, to enhance their electrochemical performance [65]. These composites offer several advantages that make them attractive for SCs. Metal compounds, conducting polymers (CPs), and carbonaceous materials have all been combined with MXenes to afford a variety of MXene-based composites [66]. As a result, a synergistic effect was achieved, whereby MXenes' exceptional electronic conductivity contributed to the quick movement of electrons, increased the exposed surface area, and stabilized the structure of the materials [67]. These materials also prevent the restacking of the MXene nanosheets by serving as a spacer and increasing the interlayer gap. Ions become more

accessible and travel faster as a result. MXene-based nanocomposites have demonstrated superior electrochemical performance compared to both pure MXene and active materials. Different kinds of MXene-based composites as they are applied in energy storage devices are shown in Fig. 4.

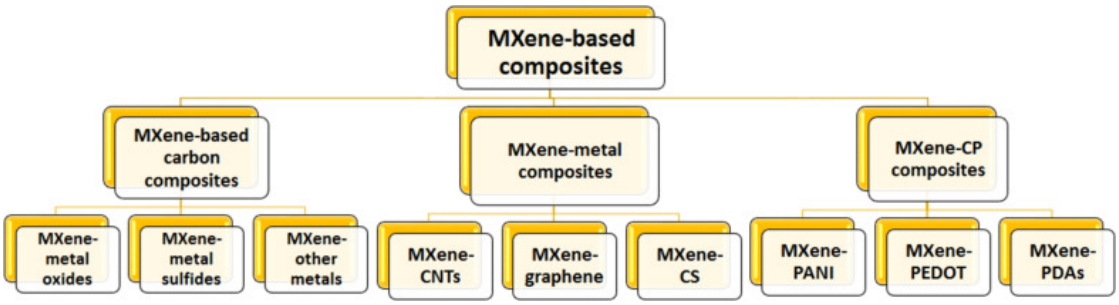

Fig. 4. MXene-based composites as electrode materials for supercapacitors.

Through binary MXene composites, the following advantages can be obtained:

5.1.1. Enhanced electrical conductivity

One of the primary motivations for synthesizing MXene binary composites is to improve the electrical conductivity of MXenes. Pristine MXenes have good conductivity, but when incorporated with highly conductive materials like carbon nanotubes, graphene, or metal nanoparticles to make composites, their overall electrical conductivity can be significantly increased [68]. This results in improved charge transfer kinetics and reduces internal resistance, leading to enhanced supercapacitor performance. For instance, by using direct synthesis to uniformly intercalate a conductive coordination polymer, Ni-BTA, onto the abundant —O termination on the surface of $Ti_3C_2T_x$ nanosheets, Kim et al. developed a unique intercalation technique [69]. Ni-BTA is an efficient charge carrier transport channel because it is composed of a nickel center and 1,2,4,5-benzenetetetramine (BTA) organic ligand with 1D-stretched localized π-d electrons. The Ni-BTA/MXene film has 2.1 times the specific capacitance of the pure $Ti_3C_2T_x$ film at 5 mV s^{-1}. After 10,000 cycles, the capacitance retention reached a maximum of 94.6 % [69].

5.1.2. Increased pseudocapacitance

MXenes are known for their high pseudocapacitance, which arises from Faradaic redox reactions at their surface [70]. When combined with other materials like transition metal oxides or conductive polymers in a binary composite, the pseudocapacitance can be further enhanced. This leads to higher specific capacitance values and improved energy storage capabilities for supercapacitors and other electrochemical devices. For instance, MXene, Ti_3AlC_2 and conducting polymers were used in an investigation by on the production of thin and flexible electrodes. The use of conducting polymer helped to increase not only pseudocapacitance behavior of MXene but also the charge transfer resistance [71].

5.1.3. Synergistic effects

The combination of MXenes with other materials can lead to synergistic effects that result in improved electrochemical performance [72]. For example, MXenes can provide a high surface area for ion adsorption, while another component can introduce specific chemical reactivity or

a unique charge storage mechanism. This synergy often translates into higher overall performance. For instance, Yang et al. [73] used the electrophoretic deposition method to produce $Ti_3C_2T_x$/CNT films on graphite paper as electrode material for SCs as shown in Fig. 5a. At 1 A g^{-1}, the specific capacitance of the $Ti_3C_2T_x$/CNTs film was evaluated to be 134 F g^{-1} (Fig. 5b), which is around 1.5 and 2.6 times respectively more than the pure $Ti_3C_2T_x$ (85 F g^{-1}) and CNTs (50.7 F g^{-1}) films. Because ions can now more easily reach the inner layer of the $Ti_3C_2T_x$/CNTs film, the electrode demonstrated impressive cycling stability with no capacitance decline over 10,000 cycles (Fig. 5c). The assembled symmetric device delivered capacitance of 55.3 F g^{-1} at 0.5 A g^{-1} and an energy density of 0.56 Wh kg^{-1} at 5 A g^{-1} with a power density of 416.7 W kg^{-1}, demonstrating the excellent performance of the electrode binary electrode [73].\

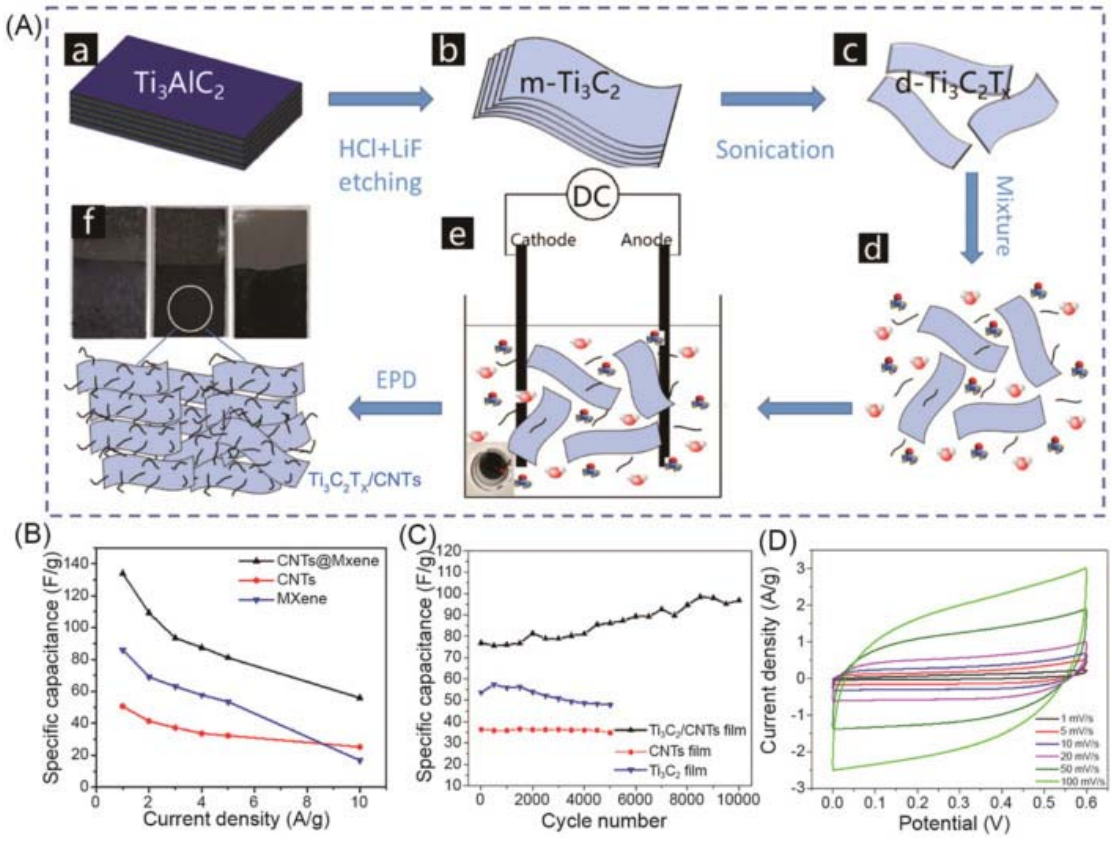

Fig. 5. (A) Synthesis process and morphology of $Ti_3C_2T_x$/CNTs (B) Specific capacitance at different current densities (C) Cycling stability of the electrode materials (D) CV curves of $Ti_3C_2T_x$/CNTs at different scan rates [73].

5.1.4. Stability and durability

MXene binary composites can exhibit an improved stability and long-term durability compared to pristine MXenes. The addition of another material can help mitigate issues like MXene restacking, which can reduce the effective surface area for charge storage [74]. Additionally, certain components can provide mechanical stability to the composite, making it more robust during charge-discharge cycles. For instance, by filtering alkalized $Ti_3C_2T_x$ and holey graphene oxide (HGO) dispersions and then mildly annealing the membranes, Fan et al. [75] designed flexible $Ti_3C_2T_x$/holey graphene (MX-rHGO) membranes. The findings indicate that porous

graphene formed a densely linked network of nanopores that enhanced ion transport and shortened the electrolyte ion transport path by acting as a spacer to prevent the $Ti_3C_2T_x$ from self-stacking [75].

5.1.5. Compatibility with various electrolytes

MXene binary composites can be designed to be compatible with different types of electrolytes, including aqueous and non-aqueous solutions, making them versatile for a variety of electrochemical applications. MXene binary composites have shown great promise in improving the electrochemical performance of MXenes in applications such as supercapacitors, batteries. Their ability to combine the strengths of MXenes with other materials to fabricated high-performance hybrid materials position them as a crucial area of research in the field of energy storage, including supercapacitors [76].

6. MXene ternary composites

Unlike binary MXene composites with two components, MXene-based ternary composites consist of MXenes along with two other materials, are a subject of significant interest in the field of electrochemical energy storage and conversion [77]. These composites are highly promising for improving the electrochemical performance of various devices, such as supercapacitors and batteries. MXene-based ternary composites often exhibit a higher energy density compared to binary composites or pure MXenes. This enhancement results from the synergistic combination of different materials, each contributing unique charge storage mechanisms, such as double-layer capacitance, pseudocapacitance, and faradaic reactions. The incorporation of two additional components allows for a more efficient utilization of the available surface area. As a result, ternary composites can store more charge per unit mass or volume, leading to higher specific capacitance or capacity in supercapacitors and batteries [78]. The various materials in the composite can be optimized to achieve a balance between fast charge-discharge rates and high energy storage capacity, making them suitable for supercapacitor applications. In addition, the combination of materials in ternary composites can mitigate degradation mechanisms that might affect the long-term stability of the supercapacitor. This results in longer cycle life and sustains electrochemical performance [79]. Furthermore, the inclusion of multiple materials in the ternary composite can offer additional functions, such as enhanced mechanical strength, thermal stability depending on the specific components used. The electrochemical performance of MXene-based ternary composites is highly promising, and ongoing research aims to further optimize their design and composition to address the evolving needs of various energy storage and conversion technologies. These composites represent a significant advancement in improving the efficiency and functionality of electrochemical devices in a sustainable and environmentally friendly manner [80].

6.1. Ternary composites of MXenes and carbonaceous materials

Ternary composites of MXenes and carbonaceous materials for supercapacitors are a subject of significant research and development in the field of energy storage. These composites combine MXenes, carbon-based materials, and often a third component, such as metal oxides or conductive polymers, to enhance the electrochemical performance of supercapacitors [81]. The materials composed of elemental carbon can take on several forms, including amorphous, graphite, diamond and so on. Excellent physicochemical characteristics can be found in carbon-based materials, including good mechanical, optical, and electrical qualities. As a result, a lot of carbon-based components are added to the MXene-based composites to increase their

conductivity, promote flexibility, enhance electrochemical performance, etc. Recently, carbon compounds that have attracted the greatest attention are graphene, carbon nanotubes (CNTs) and mesoporous carbon. Some examples are given below:

6.2. MXene/carbon/conducting polymer ternary composites

The conducting polymers that are being investigated the most for use in supercapacitor devices are polyaniline (PANI), poly(3,4-ethylenedioxythiophene) (PEDOT), polypyrrole (PPy), and polythiophene (PTh). Their intrinsic conductivity is high with a lower band gap (1-3 eV) than ordinary polymers (10 eV). Additionally, these polymers have a variety of morphologies, distinct doping and undoping behaviors, and a relatively quick charge and discharge rate [82]. Cai et al. [83] presented a novel and straightforward method for obtaining ternary material (MXene-CNT/PANI) and examined the supercapacitive capabilities of the material. PANI was uniformly coated across the surface of the multi-walled carbon nanotubes (MWCNTs) using the in-situ polymerization approach, resulting in the tubular-like nanocomposite (CNT/PANI). After evenly combining the CNT/PANI nanocomposite solution with the MXene ($Ti_3C_2T_x$) suspension, a vacuum-assisted suction filtration was used to obtain the MXene-CNT/PANI ternary material. The CNT/PANI nanocomposite may enhance the ion migration performance in the composite electrode by preventing the re-stacking propensity of MXene nanosheets, while the conductive MXene in the ternary composite can efficiently speed up the transmission of electrons. The combination of these individual chemicals has a synergistic effect that allows MXene-CNT/PANI to exhibit better specific capacitance (429.4 F g^{-1}) and outstanding rate capability (84.4 % retention at 10 A/g). Moreover, the as-assembled asymmetric supercapacitor exhibits exceptional cycling stability, with 8.8 % capacitance degradation after 10,000 cycles, and a notable energy density of 11.3 Wh kg^{-1} at a power density of 500.0 W kg^{-1} [83].

Wang et al. [84] designed a 3D interconnected and hydrate ion-permeable MXene/graphene nanotube (MG) composite sheet. The combined effects of the uniformly distributed pores in GDY-NTs and the horizontal-vertical 3D-intercalation improved the capacitance and rate performance of MG films. The capacitance of the $Ti_3C_2T_x$/GDY-NTs composite film significantly improved to 337.4 F g^{-1} in comparison to the pure $Ti_3C_2T_x$ film (230.8 F g^{-1}), and the rate capacity rose to 73 % at 100 mV s^{-1}. An asymmetric solid-state flexible SC with an energy density of 19.7 Wh kg^{-1}, a power density of 750 W kg^{-1}, and an 88.2 % capacitance retention rate at 10,000 cycles at 8 A g^{-1} was obtained [84].

In another study, a ternary composite comprising carbon fiber (CF), MXene and PANI was constructed and used as electrode material for supercapacitor application [85]. An excellent capacitance of 193.75 F g^{-1} at 1 A/g and good stability of 89 % retention rate after 2000 charge/discharge cycles were achieved, according to characterization of electrochemical performance. The curve profile of the ternary composite, owing to the synergistic interaction between PANI and MXene, was similar to that of CF@PANI composite fibers. Because of the special porous nanostructured growth layer topography, samples with a co-growing duration of 2 h (M3-P-2H) had the maximum encircled area and current responsiveness, and the redox peak signal enhanced. The specific capacitance of the CF@MXene/PANI composite decreased as current density grew from 0.25 to 10 A/g, whereas M3-P-2H's specific capacitance outperformed other samples over the whole current density range [85].

Furthermore, Wang and co-workers [86] developed a novel approach that forms a flexible film with a sandwich structure by merging the ternary components of polypyrrole (PPy), MXene, and reduced graphene oxide (rGO) into one electrode. The resultant rGO/MXene-PPy

composite electrode has strong mechanical qualities, high conductivity, and pseudocapacitance. Apart from its capacitive contributions, the PPy acts as a coating layer that considerably shields MXene from oxidation and prevents face-to-face restacking of the 2D nanosheets. As a result, the rGO/MXene-PPy electrode shows excellent rate performance, with 67.3 % capacitance retention at an enhanced current density of 10 A g^{-1}, and a high specific capacitance of 408.2 F g^{-1}. Xie et al. successfully prepared a ternary PANI/graphitic carbon nitride (g-C_3N_4)/MXene (PCM) composite via in situ chemical polymerization and vacuum-assisted filtering. When compared to the individual components, the resultant ternary composite has superior physicochemical characteristics and morphologies, which improve its electrochemical performance. At 5 mV s^{-1}, the PCM composite exhibits a high specific capacitance of 570 F g^{-1}. More significantly, compared to single electrodes, the PCM electrode shows superior electrochemical stability at high scan rates [86].

Recently, the work of Vigneshwaran and colleagues examined a flexible film of V_2C-PPy-PdO prepared by electrodeposition method [87]. The V_2C-PPy-PdO electrode architecture combined highly conductive 2D V_2C MXene nanosheets with a 3D framework of PPy and PdO, resulting in a highly efficient network with outstanding conductivity and structural stability (Fig. 6). The performance of the ternary electrode showed an impressive capacitance of 487F g^{-1} at 1 A g^{-1}. The constructed two-electrode device delivered an energy density of 64.5 Wh kg^{-1} and a power density of 980.9 W kg^{-1} with an excellent cycle life exceeding 10,000 cycles. The study underscores the potential of the ternary V_2C-PPy-PdO composite electrode in supercapacitor application [87].

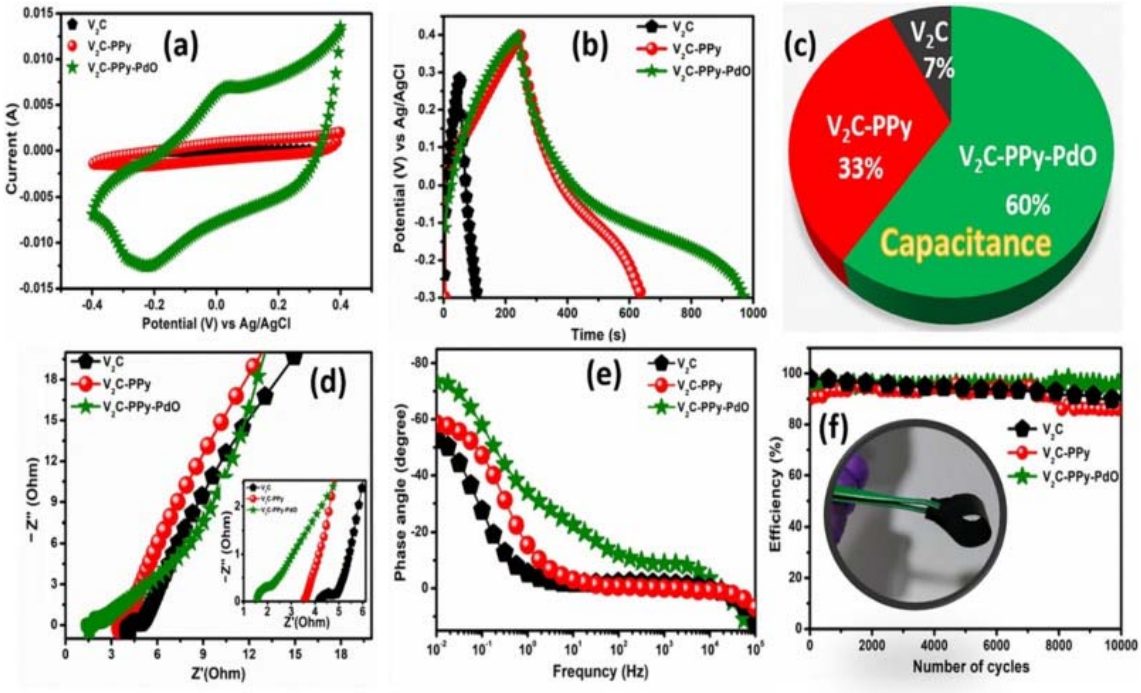

Fig. 6. CV curves of V_2C, V_2C-PPy, and V_2C-PPy-PdO at 10 mV s^{-1} (b) GCD curves at 1 A/g, (c) Percentage contributions of capacitance of the electrodes (d) Nyquist plots from 0.01 Hz to 100 k Hz frequencies (inset: focusing on the high frequency region), (e) Bode plots, and (f) Cycling stability at 3 A/g for 10,000 cycles [87].

6.3. Ternary nanocomposites of MXenes and inorganic materials

Ternary nanocomposites of MXenes and inorganic materials offer several advantages for improving supercapacitor performance. These materials combine the strengths of MXenes, which have high electrical conductivity and large surface areas, with inorganic materials that can provide additional charge storage mechanisms and other benefits [85].

6.3.1. MXene-metal oxide ternary composites

Metal oxides have garnered significant interest as a possible alternative to conventional pseudocapacitive materials because of their relatively low cost, high theoretical capacity, and environmental friendliness. To achieve high capacity and extended stability for supercapacitors, the composite of metal oxides with a distinctive nanostructure on conductive MXene matrix highly promising This is because it lowers contact resistance, enhances the transfer of ions, and guards against capacity attenuation and structural deformation. For instance, Lu et al. [88] prepared a ternary composite of PANI@TiO_2/$Ti_3C_2T_x$ with a hierarchical structure for high-performance electrochemical supercapacitors. The ternary composite with hierarchical PANI@TiO_2/$Ti_3C_2T_x$ demonstrates a high specific capacitance of 435.4 F cm^{-2} at 0.5 A g^{-1} in KOH solution and 188.3 F g^{-1} at 10 mV s^{-1}, which was almost twice that of TiO_2/$Ti_3C_2T_x$. Additionally, at a current density of 1 A g^{-1}, it exhibits exceptional cycle stability of 94 % of the starting value even after 8000 cycles. The hierarchical architecture and the synergistic effect of mixing PANI nanoflakes with TiO_2/$Ti_3C_2T_x$ composite are responsible for the improved electrochemical performance [88].

A facile hydrothermal method was employed to synthesize a $Co_3V_2O_8$/Co_3O_4/Ti_3C_2Tx composite, which was grown on Ti_3C_2Tx's surface through strong Co—F bonds [89]. This results in a high specific capacitance, rate capability, and cycling stability. The device based on this ternary composite and active carbon, has a high energy of 84.0 μWh·cm^{-2} at a power density of 3.2 mW·cm^{-2}, and excellent cycling durability with 87.0 % after 20,000 cycles [89]. Chavan et al. [90] presented a simple, low-cost, two-step deposition method to synthesize a ternary composite electrode material based on a mixture of MXene with metal oxides, namely MnO_2 and CuO, to fabricate supercapacitors with high gravimetric capacitances. The ternary nanocomposites are porous, which improves electrochemical performance by giving electrolyte ions lots of pathways and access. With a specific capacitance of 924.16 F g^{-1} at a current density of 10 mA/cm^2 and good cycling retention of 77.92 % of its original specific capacitance in 1 M Na_2SO_4 electrolyte over 4000 cycles. Moreover, the asymmetric device shows a specific capacitance of 25.0 F g^{-1} and an energy density of 3.5 W h/kg and a maximum power density of 571.2 W kg^{-1} [90].

Iyer et al. prepared a ternary composite of bismuth antimonate (BSO), GNF and MXene via hydrothermal process [91]. With a specific capacitance of 819 F g^{-1} at 1 A g^{-1} and a capacity retention of 94 % after 5000 cycles, the electrode showed battery-type behavior. After 20,000 cycles, an asymmetric supercapacitor device with activated carbon electrodes and a BSO-based nanocomposite had a favorable specific capacitance of 147.8 F g^{-1}. It also demonstrated a capacity retention rate of 90.6 %. The accordion-type MXene structure and the conductive components GNF are responsible for the improved performance [91].

Xie and colleagues [92] used a vacuum-assisted filtering technique to fabricate a PANI/MoO_x nanowires composited with MXene (PMM) film electrodes, which not only reduced the restacking of the MXene matrix but also increased the number of ion transport channels and

storage spaces. When utilized as supercapacitor electrodes, the PMM composite film containing 20 wt% PANI/MoO_x nanowires (PMM-20) delivered a high specific capacitance of 450 F g^{-1} at 5 mV s^{-1} and a high capacitance retention of roughly 91.5 % after 10,000 cycles. Furthermore, the symmetric supercapacitors based on PMM-20 composite film electrodes show an energy density of 19.53 Wh kg^{-1} at a power density of 1610.11 W kg^{-1} [92].

Moniruzzaman and co-workers [93] developed a simple hydrothermal strategy for the synthesis of 3D-0D-2D-ternary nanocomposite consisting of SnO_2 nanospheres (3D) and carbon dot (0D)-embedded $Ti_3C_2T_x$ nanosheets (2D) for hybrid supercapacitor devices. Highly conducting 0D CDs were deposited on MXene, changing both its surface area and its ability to store surface charge. The entire electrode arrangement is stabilized by the homogeneous development of spherical SnO_2 over the MXene sheets. In a three-electrode system, the SnO_2-stabilized carbon dot-embedded MXene nanocomposite reached a maximum specific capacitance of 1074 F g^{-1}. An asymmetric supercapacitor device was used to show the ternary electrode's practical application, with SnO_2/CDs@MXene serving as the positive electrode. The device exhibited functionality across an extensive operating potential range of 0–2.0 V, with a maximum energy density of 51.11 W h/kg [93].

Furthermore, it is possible to improve supercapacitor performance by utilizing the synergistic structure of MXene-linked hierarchical porous and hollow carbon nanofibers incorporating metal oxides. Recently, Donthula et al. [94] synthesized Co_3O_4-coated hollow MXene-embedded carbon nanofibers (HMCNF) by electrodeposition method to utilize synergetic effects from fibers, metal oxide, and MXene (Fig. 7a). As seen in Fig. 7(b–c), the FESEM pictures showed a uniform and even surface on the core-shell nanofibers without any obvious bead formations. Furthermore, the presence of Co_3O_4 nanopillars on the surface of HMCNFs causes a wider nanofiber diameter, as seen in Fig. 7(d–e). The number of active sites is increasing because of this surface area increase. The results of the EDS analysis for the HMCNF and Co_3O_4/HMCNF samples are shown in Fig. 7g and f. The examination verifies that N, O, Ti, and C elements are detectable on both surfaces of the Co_3O_4/HMCNF sample, as well as the presence of Co on its surface. The ternary composite demonstrated fast reaction kinetics and high conductivity, enhancing electrochemical performance. This led to an exceptional specific capacitance of 374.4 F g^{-1} at 0.5 A g^{-1}, together with a noteworthy cycle stability of 88.5 % capacity retention over 5000 cycles. Moreover, the symmetrical device constructed using this ternary electrode showed remarkable energy storage properties, producing a notable rate capability of 63.9 % at 5 A g^{-1} and a high energy density of 52.5 Wh kg^{-1} at a power density of 1000 W kg^{-1} [94].

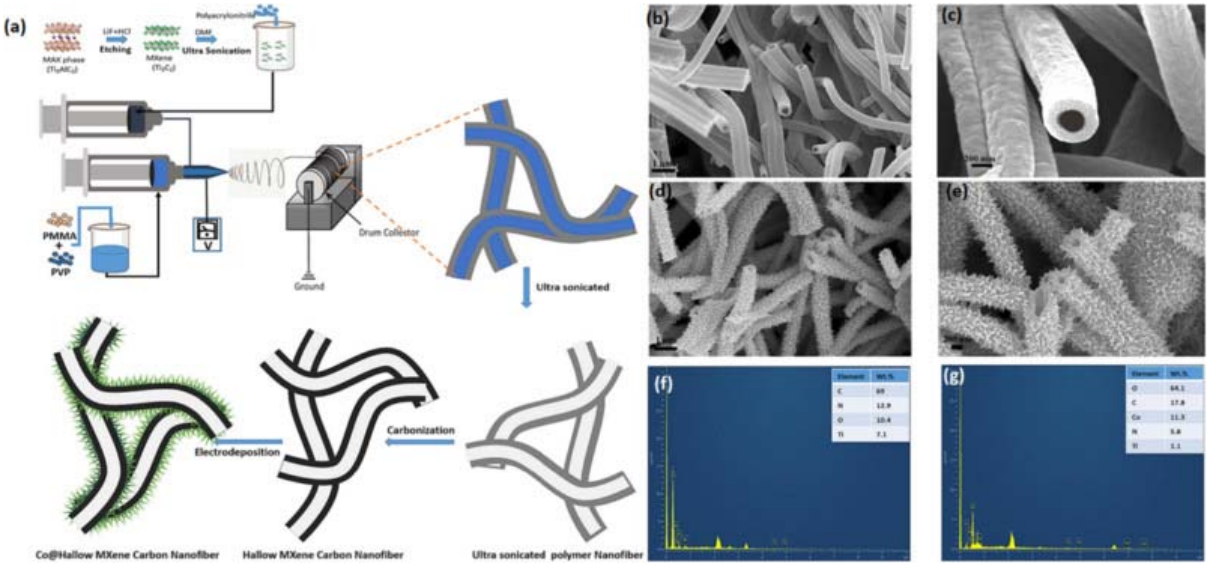

Fig. 7. (a) Schematic illustration of the synthesis of Co_3O_4/HMCN. SEM images of (b, c) HMCNF (d, e) the SEM images of Co_3O_4/HMCNF composite superstructures, (f, g) EDS spectrum obtained from HMCNF and Co_3O_4/HMCNF composite [94].

A hydrothermal and in-situ polymerization technique was devised by Shahid et al. to produce CeO_2/MXene/PANI-based nanocomposites. CeO_2/MXene/PANI 80 %:20 % (CMP1), CeO_2/MXene/PANI 60 %:40 % (CMP2), and CeO_2/MXene/PANI 40 %:60 % (CMP3) were the three composites that were prepared. The ideal electrode material for pseudocapacitors is the CMP3 composite, which showed decreased band gap energy, high capacitance, dielectric constant, and low charge transfer resistance. It also maintained 91 % capacitance after 6000 cycles [95].

Recently, a scalable hydrothermal and in-situ polymerization technique was reported by Shahid et al. [96] for the synthesis of CeO_2/MXene/PANI-based nanocomposites. Three ternary composites were prepared: (CeO_2/MXene)/PANI 80 %:20 % (CMP1), (CeO_2/MXene)/PANI 60 %:40 % (CMP2), and (CeO_2/MXene)/PANI 40 %:60 % (CMP3). To disclose the different properties and prospective applications of the synthesized materials, innovative procedures are employed for their characterization. In the optical research, the CMP3 composite shows a reduced band gap energy of up to 2.19 eV. Furthermore, this material is advantageous for capacitors due to its high capacitance and dielectric constant of 169.9. It also has the highest specific capacitance of 2247.962 Fg^{-1}, the lowest charge transfer resistance of all the as-prepared samples, an exceptional rate capability, and an outstanding cycle life, sustaining 91 % after 6000 cycles.

6.4. MXene metal sulfide ternary composites

Research on layered metal sulfides' rapid ionic conductivity has led to the creation of a tungsten disulfide-decorated $Ti_3C_2T_x$/BN nanohybrid, used as a cathode for flexible asymmetric supercapacitors. By decreasing the sheet restacking, the MXene/functionalized BN heterostructure displayed a greater surface area. In order to produce a flexible asymmetric supercapacitor with a specific capacitance of 1318 $F \cdot g^{-1}$ at 1 A g^{-1} in 1 M KOH, the study integrated WS_2 over MXene/functionalized BN sheets. A PVA–KOH–KI gel electrolyte was used to build the supercapacitor, with KI serving as a redox component. The findings

demonstrated an extraordinary 140 F g^{-1} specific capacitance with a good energy density of 19.4 Wh kg^{-1} at 1 A g^{-1}, as well as 84 % capacitance retention after 10,000 cycles. The gadgets also showed off how well-designed LED lights might be, indicating a potential use for them in portable electronics [97].

Furthermore, a direct hydrothermal procedure was used by Hussain and co-workers [98] to prepare porous WS_2 nanosheets-interconnected MXene/GO (WS_2@MXene/GO) nanocomposites for electrochemical supercapacitors. At 2 A/g applied current, the constructed WS_2@MXene/GO nanocomposites electrode yielded an excellent specific capacitance of around 1111 F·g^{-1}. Additionally, the asymmetric device made with the nanocomposite had remarkable cycling stability and a high specific energy of 114 Wh kg^{-1} [98]. Sharma et al. studied the 1 T Metallic Vanadium disulfide/MXene/functionalized multiwalled carbon nanotubes (1 T-VS_2-MX-CNT) ternary hybrid synthesis for asymmetric supercapacitors. The study found that the interlayer spacing increased from 13.45 to 13.81 Å depending on the precursor ratio, as revealed by x-ray diffraction patterns [99].

Moreover, the optimized ternary composite (VS_2-MX-CNT-50) achieved the highest specific capacitance of 505 F g^{-1} at 0.2 A/g. In addition to preventing the MXene layers from re-stacking, the VS_2 nanosheets serve as an electron transmission pore space. The ternary electrochemical characteristics of the composite were further improved with the addition of functionalized MWCNTs, which aid in creating a conductive channel for improved ion transport [99].

Recently, Abraham et al. [100] synthesized NiFe-LDH/MoS_2/MXene nanocomposites using a two-step preparation strategy and combined them using the incipient wet impregnation technique to form a ternary nanocomposite. The excellent conductivity of MoS_2/MXene nanocomposites together with the remarkable capacity of NiFe-LDH enhanced the electrochemical efficiency of the NiFe/MM electrode for supercapacitor application. The ternary $NiFe_{60}/MM_{40}$ electrode showed improved specific capacity of 349.49 mAh g^{-1} at 1 A g^{-1} and battery-type behavior. At an energy density of 65.9 Wh kg^{-1}, the $NiFe_{60}/MM_{40}$//MM hybrid supercapacitor device produced an impressive power density of 898.9 W kg^{-1}. The remarkable electrochemical performance of the ternary nanocomposite is a result of the stacked beneficial interaction among the three components that constitute the ternary composite [100].

6.5. MXene metal ternary composites

Because of their exceptional properties including high electrical conductivity, metals have been utilized to modify the properties of other materials. Liu et al. developed a supercapacitor electrode using $NiCo_2Se_4$/MXene, enhancing the performance of pristine MXene. The composite achieved a specific capacitance of 953.8 Fg^{-1} and 93.9 % cycle stability after 3000 cycles. The electrode also showed high energy density at 22.4 Wh kg^{-1} and retained 60.8 % of its capacitance after 10,000 cycles. The addition of highly conductive MXene improved the electrode's electrochemical performance [101].

In some cases, metal-organic frameworks (MOFs) can serve as a template to produce MXene/metal ternary composites for supercapacitors. To reduce the aggregation of $CoSe_2/Ni_3Se_4$ nanosheets, Yang et al. [102] prepared ZIF-67-derived $CoSe_2/Ni_3Se_4$ nanosheets that were attached vertically on the MXene nanosheets substrate (Fig. 8). In the meantime, the addition of highly conductive MXene improves holistic conductivity, which stops MXene flakes from restacking. Moreover, the close coupling of MXene and $CoSe_2/Ni_3Se_4$ nanosheets

accelerates the rate of charge transfer and increases the structure's robustness. As shown in Fig. 9, the honeycomb-like MXene@$CoSe_2$/Ni_3Se_4 electrode material for supercapacitors achieves an exceptional capacitance retention rate of 80 % after 5000 cycles and a high specific capacitance of 283 mAh g^{-1} at 1 A g^{-1} [102].

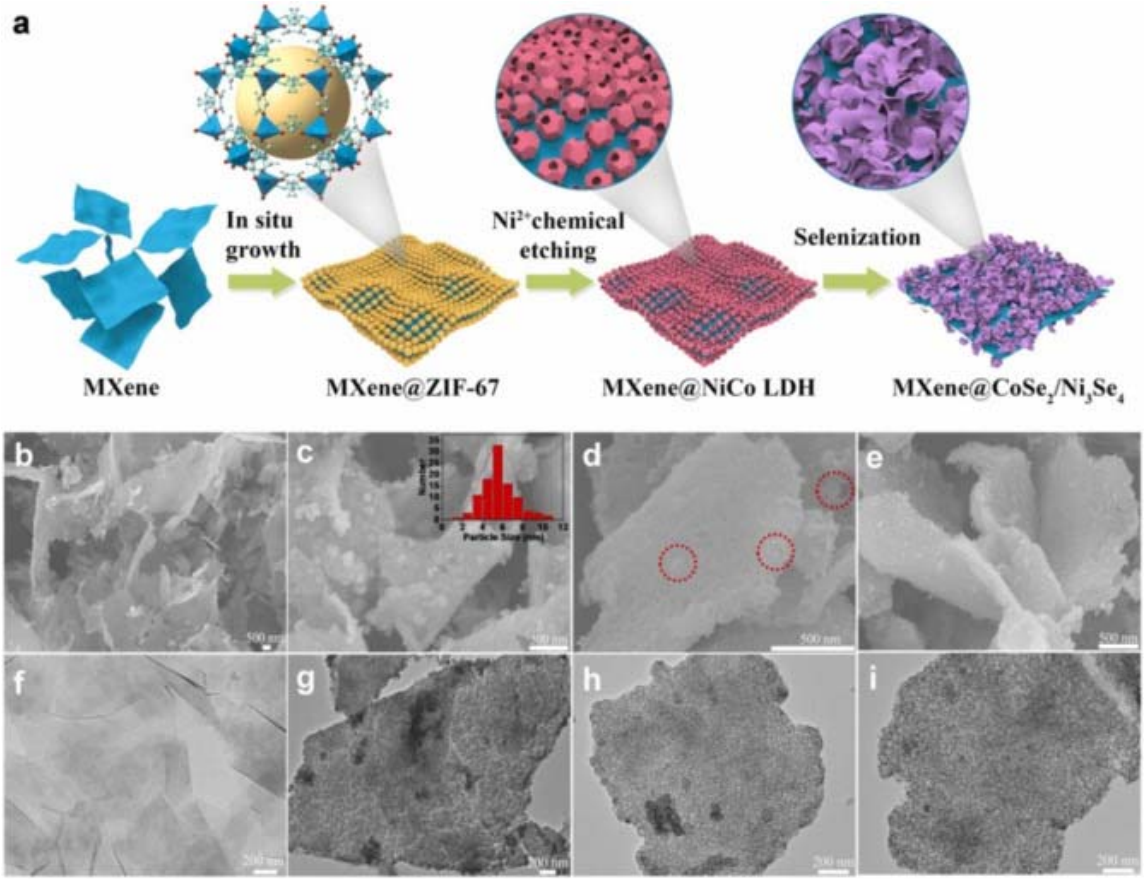

Fig. 8. (a) The synthesis procedure of 2D MXene@$CoSe_2$/Ni_3Se_4 nanosheets (b-i) SEM and TEM images of Ti_3C_2 MXene nanosheets, MXene@ZIF-67, MXene@NiCo LDH, and MXene@$CoSe_2$/Ni3Se_4 nanosheets respectively [102].

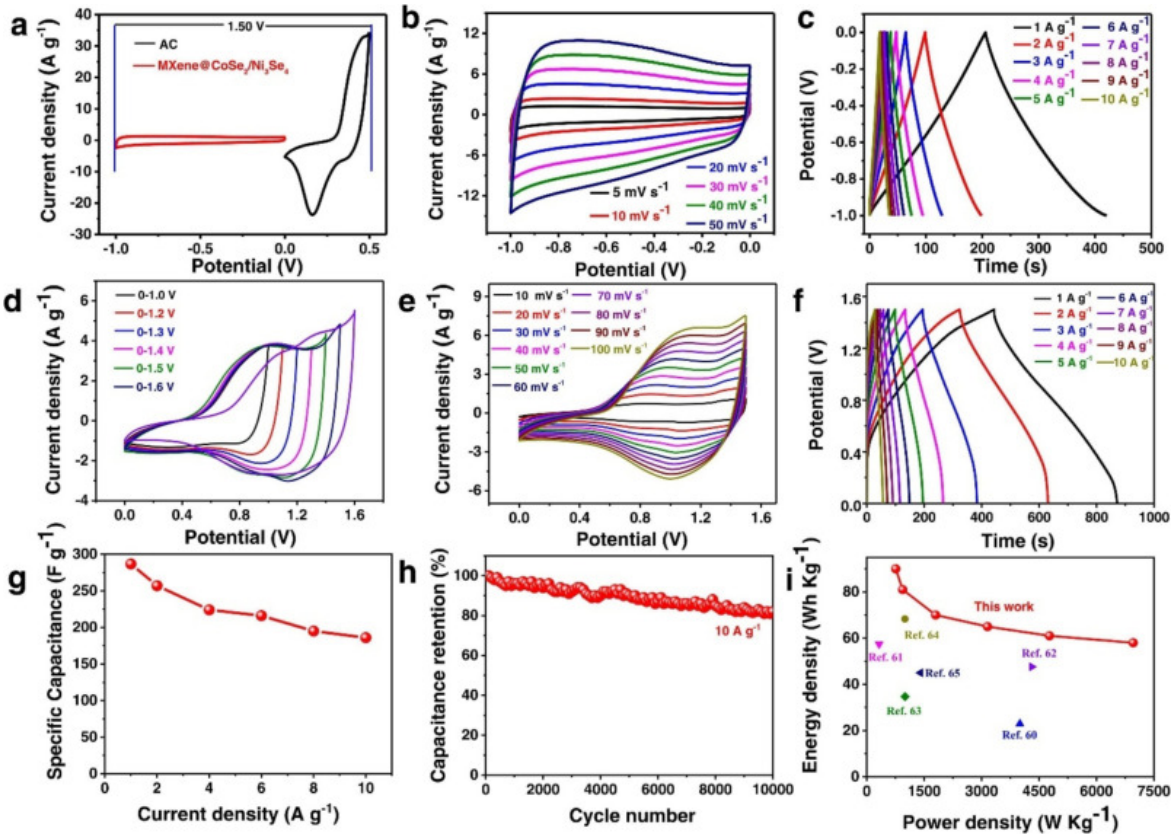

Fig. 9. (a) Electrochemical performance of an MXene@$CoSe_2$/Ni_3Se_4/AC asymmetric supercapacitor, (b) CV curves of MXene@$CoSe_2$/Ni_3Se_4 electrodes in a three-electrode (d–f) Comparison of CV and GCD curves at different scan rates and current densities, (g) Specific capacitance of the device at different scan rates, (h) Cycling stability tests at different cycle numbers (i) Ragone plot of the as-assembled ASC device and some reported results [102].

By employing a facile hydrothermal technique, Javed et al. reported heterostructure bimetallic sulfide layered $Ti_3C_2T_x$–MXene (HS–NCS@MXene) and examined its electrochemical performance as electrode materials for possible use in hybrid supercapacitors. By producing an ultrahigh capacitance of 2637 F g^{-1} (1582C g^{-1}) at 2.5 A g^{-1} with consistent cycling life (96 %) over 10,000 cycles, an improved HS–NCS@MXene demonstrates impressive pseudocapacitive performance. The fabricated hybrid device incorporating HS–NCS@MXene//AC–AHSC afforded a high capacitance of 226 F g^{-1} at 1.5 A g^{-1} with high energy density of 80 Wh kg^{-1} at 1196 Wkg^{-1} [103].

Samal et al. also reinforce new beneficial opportunities and scale up exploitation of the bifunctional electrodes by rational design of bimetallic $NiCoSe_2$/2D $Ti_3C_2T_x$ MXene for a high-performance flexible supercapacitor. At a power density of 0.2 kW kg^{-1}, the heterostructure device exhibits a specific energy density of 32.05 Wh kg^{-1}, while maintaining an energy density of 15.39 Wh kg^{-1} at power density of 0.92 kW kg^{-1} [104].

6.6. Ternary nanocomposites of MXenes, inorganic and other materials

In one study, PANI@TiO_2/$Ti_3C_2T_x$ ternary composite was prepared by a combination of in-situ polymerization and hydrothermal procedure and evaluated for electrochemical

performance [88]. In this work, the $Ti_3C_2T_x$ nanosheet is an active material with a high number of electrochemical active sites for easy incorporation of other materials in the composite. The improved electrochemical performance of the composite was attributed to the PANI and TiO_2 nanoflakes and nanoparticles, respectively. The conductive material's surface area was increased, and the pseudo capacitive effect was pronounced with the help of the microstructures of PANI and TiO_2. It is noteworthy to notice that the hierarchical PANI@TiO_2/$Ti_3C_2T_x$ ternary composites-based specific capacitance (188.3 F g^{-1}, scan rate: 10 mV s^{-1}) was twice as high as TiO_2/$Ti_3C_2T_x$ [88]. On the other hand, at 0.5 A/g of current density, the areal capacitance in a KOH solution was determined to be 435.4 F/cm^2. The superior electrochemical performance and cycling stability of the composite electrodes were linked to the PANI nanoflakes' harmonic interactions with TiO_2/Ti_3C_2Tx hybrids and their nanostructures [88].

Kshetri et al. used a highly flexible conductive MXene-carbon nanofiber mat (MX-CNF) with a cobalt metal-organic framework (Co-MOF) to create high-performance flexible wearable hybrid supercapacitors (FW-HSCs). Co-MOF@MX-CNF and MnO_2@Co_3O_4-PC@MX-CNF were used to create the composite electrodes. 426.7 F g^{-1} of specific capacitance and 475.4 mAh g^{-1} of specific capacity were displayed by the improved electrode. At a power density of 832.4 W kg^{-1}, the FW-HSC demonstrated long-term stability and an energy density of 72.5 Wh kg^{-1}. These results imply that FW-HSCs could be useful as power sources for a range of wearable electronics uses [105].

In the work of Abraham et al. [106] a ternary nanocomposite $NiFe_x$/MM100–x, which integrates NiFe-LDH, MoS_2, and MXene was prepared in a two-step synthesis method (solvothermal and incipient wetness impregnation) (Fig. 10). The ternary composite material exhibits remarkable electrical conductivity and high capacity, rendering it a promising electrode material for high-end battery-style supercapacitors. The $NiFe_{60}$/MM40 composite demonstrated a specific capacity of 349.49 mAh g^{-1} at 1 A g^{-1}. A hybrid supercapacitor device was designed using $NiFe_{60}$/MM40//MM as the positive electrode and MM as the negative electrode, delivering an energy density of 58.66 Wh kg^{-1} and exhibiting exceptional cyclic stability with 845 capacitance retention 5000 cycles at 10 A g^{-1} [106]. A summary of the performance of ternary MXene composites is given in Table 1.

Table 1. MXene ternary composites for enhanced supercapacitor applications.

Ternary composite	Material	Electrolyte	Capacitance/capacity	Energy density (Wh/Kg)	Power density (W/Kg)	Capacitance/capacity retention/cycle number (%/cycles)	Ref
Carbon-based	PANI@rGO/MXene	1 m H_2SO_4	45.62 F g^{-1}	4.68	25.48	84/10000	[107]
	rGO/CNFs/$Ti_3C_2T_x$	6 M KOH	2440 F cm^{-3} @1 A cm^{-3}	20.5 mW cm^{-3}	0.25 W cm	93.75/6000	[108]
	$Ti_3C_2T_x$/$Ti_3C_2T_x$ quantum dots/rGO	PVA/H_2SO_4	542 F c^{-3} @0.25 A cm^{-3}	16.6 mWh cm^{-3}	450 mW cm^{-3}	96.6/5000	[109]
	MXene/Ag NWs/cellulose	PVA/H_2SO_4	505 F g^{-1} at 10 mV s^{-1}	–	–	90.9/500	[110]
	g-C_3N_4/Ti_3C_2/FeOOH		71.26 F cm^{-3}/10mVs^{-1}	77.12 mW h cm^{-3}	≈6000 mW cm^{-3}	85.2/10,000	[111]
	MXene-CNT/PANI	1 M H_2SO_4	429.4 F g^{-1} at 1 A/g			93/10000	[83]
	PANI@MXene-CNTs films	3 M H_2SO_4	463 F g^{-1} at 5 mV s^{-1}	10	2808	92/10000	[112]
	PANI MXene/CNF	1 M H_2SO_4	356 F g^{-1} at 0.5 Ag^{-1}			91/5000	[113]
	MXene@NPSi@NCNFs	1 M $LiPF_6$ in EC/EDC/FEC	24 F g^{-1}, 10 mV s^{-1}	59	9.6	90/8000	[114]
Inorganic materials	Co_3O_4–MXene/rGO aerogel	6 m KOH	345 F g^{-1} @1 A g^{-1}	8.25	159.94 W kg^{-1}	85/10000	[115]
	Fe_3O_4/MXene/rGO	5 m LiCl	45.8 F g^{-1} @0.2 A g^{-1}	–	–	82.1/5000	[116]
	Ni_3S_2/FL-$Ti_3C_2T_x$/Ni	3 m KOH	1752 mF cm^{-2} @1 mA cm^{-2}	32.7 μWh cm^{-2}	8.0211 mW cm^{-2}	81.5/5000	[117]
	TiO_2/C-$Ti_3C_2T_x$/NiO	1 m KOH	92 mAh cm^{-3} @1 A g^{-1}	1.04 × 10^{-2} Wh cm^{-3}	5.88 W cm^{-3}	72.1/5000	[61]
	$Mo_{1.33}C$ MXene/PEDOT: PSS	1 M H_2SO_4	1310 F cm^{-3} at 2 mV s^{-1}				[118]
	WS2-$Ti_3C_2T_x$/BN	PVA–KOH–KI	140 F g^{-1} @1 A g^{-1}	19.4	997.7	84/10000	[97]
	MXene/MnO_2/PANI	PVA/H_2SO_4	216 F g^{-1} @1 Ag^{-1}			74/5000	[108]
	MnO_2/MXene/CuO@FSSM thin films	1 M KOH	25.0 F g^{-1}	3.5	571.2	87.27/2000	[90]
	RuO_2/MXene/CNF	3 M KOH	322 F g^{-1}@1 Ag^{-1}	20.17	900	90/2500	[119]
	SnO_2/carbon dots@MXene		92 F g^{-1} at 2 A/g	51.11	8000	103/10,000	[120]
LDH	MXene@PDDA/NiAl-LDH	1 M KOH	1825.8 F g^{-1} @1 A g^{-1}	91.3	6000	99.1/5000	[121]
	$V_4C_3T_x$/NiCoAl-LDH	1 M KOH	194 F g^{-1}, 1 A g^{-1}	71.7	830	98 %, 10,000	[122]
	$NiCo_2$-LDHs @MXene/rGO aerogel	2 m KOH	332.2 mAh g^{-1} @1 A g^{-1}	65.3	14,000	92.8/10000	[123]
	MXene/GO/Ni-Mn LDH	PVA/KOH	241.9 mAh g^{-1} at 1Ag^{-}	55^{-1}	800	4000	[124]
	NiFe-LDH/MoS_2/MXene	6 M KOH	165 Fg^{-1}	58.66	800	84/5000	[106]
MOF	$Ti_3C_2T_x$/ZIF-67/CoV_2O_6	1 M KOH	0.116 F cm^{-2}, 1 mA cm^{-2}	36.27 μWh cm^{-2}	0.75 mW cm^{-2}	94.4/4000 cycles	[125]
	Ni/Co-MOF@TCT-NH_2	3 M KOH	351.3 F g^{-1} @ 0.5 A/g	28.2	7500	99.3/15,000	[126]
	Co-MOF@MXene-carbon nanofiber	PVA/KOH gel	323.3 F g^{-1} @ 1 A/g	72.5	832.4	90/10000	[105]
	MOF/MXene/NF-300	1 M KOH	222.3 F g^{-1} @ 1 A/g	46.3	746.8	118/15000	[127]

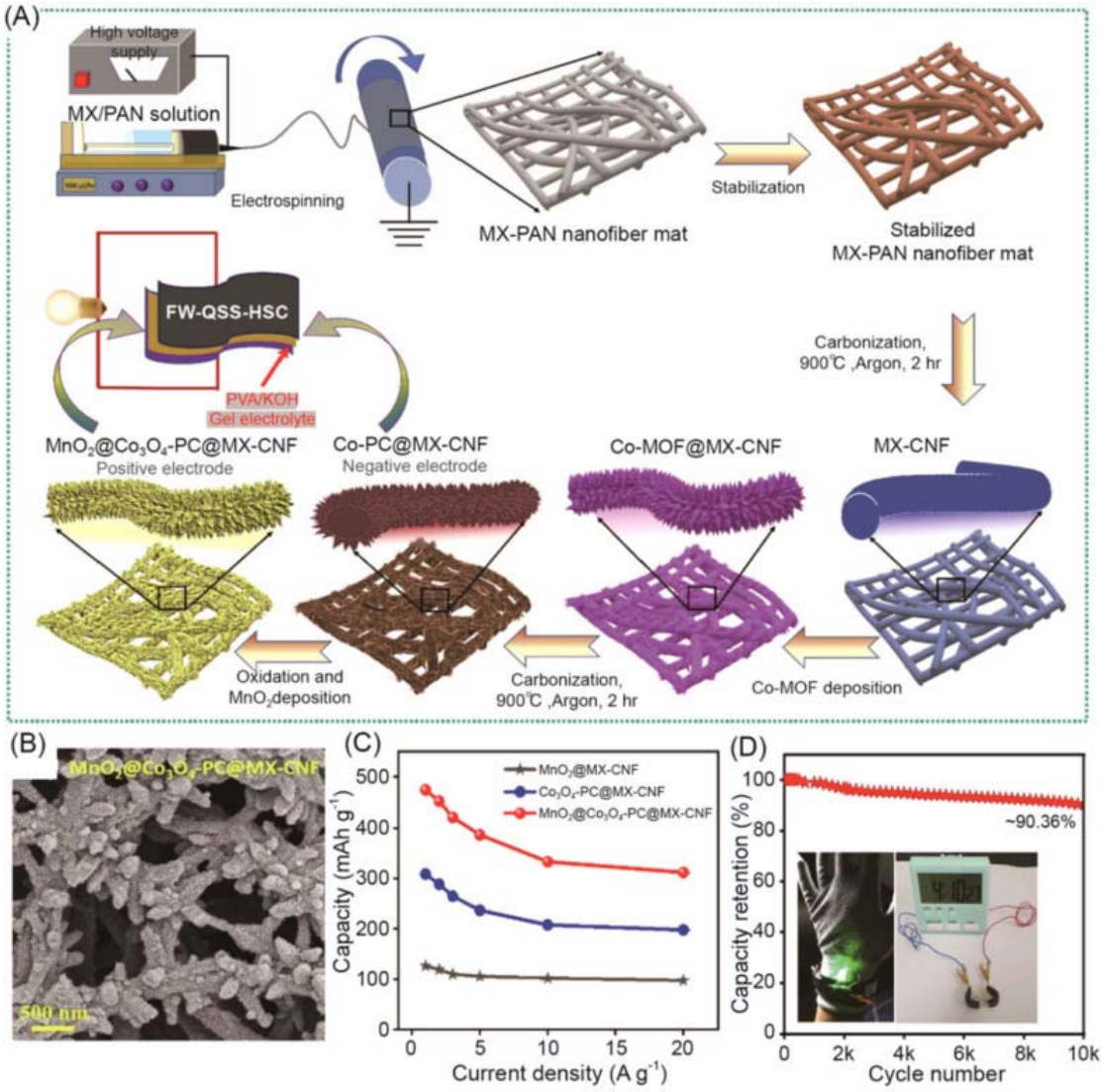

Fig. 10. (A) Synthesis procedures for MX-CNF, Co-PC@MX-CNF, MnO_2@Co_3O_4-PC@MXene-CNF, and FW-QSS-HSC device (B) FESEM images of Co3O4-PC@MXene-CNF (C) Specific capacitance vs. current density curve, (D) MX-CNF and Co-PC@MX-CNF cyclic stability performance [106].

7. MXene ternary composites for micro supercapacitors

The components of a conventional supercapacitor are a solid-state ionic conductive electrolyte or a separator that physically divides the positive and negative electrodes [128]. Since these supercapacitors are used in different applications from large load-leveling cranes and engine starters to personal mobile devices, their energy and power performance is typically normalized by the volume or mass of the electrode. On the other hand, low-power wearable electronics, microsensors, and micromechanical devices are intended to run on microsupercapacitors. In these applications, normalizing energy and power density in a particular footprint area is a more practical way to assess MSC performance, as the weight of the active materials only occupies a small portion of the substrate and the entire device. Unfortunately, MSCs are infamous for having a poor specific energy, which significantly hinders their widespread use, no thanks to restacking of MXenes [128].

To minimize this problem, ternary composites of MXenes and other active materials such as carbon, metals and metal oxides have been designed for MSCs to enhance not only the energy density but also capacitance and cycling stability. For instance, RuO_2@MXene-Ag nanowire ink was developed by Li et al. [129] via screen printing to produce micro-supercapacitors. Based on RuO_2@MXene-Ag nanowires, these supercapacitors showed exceptional mechanical and durable qualities in PVA/KOH gel electrolyte, as well as high energy density 13.5 mWh/cm at 48.5 W/cm^3. L. From the optical and SEM pictures, all printed patterns exhibit great resolution and clean edges (Fig. 11b) [129]. Furthermore, it was shown that AgNWs are evenly dispersed throughout the composite and can successfully i) stop the MXene nanosheets from restacking; ii) improve the composite's mechanical stability and conductivity [129]. Similarly, using a two-step selective screen-printing procedure, Xu et al. prepared a flexible asymmetric microscale hybrid device (MHD) (Fig. 11c). Co-Al-layered double hydroxides were selected as the positive electrode in order to balance the negative side's charge of $Ti_3C_2T_x$. The asymmetric device has a broader voltage window and areal capacitance in comparison to the symmetric MXene MSC (Fig. 11d) [130]. Thus, in 6 M KOH aqueous electrolyte, the screen-printed asymmetric MSC displays a high energy density of 10.80 μWh cm^{-2}, significantly greater than the symmetric MXene MSC (1.25 μWh cm^{-2}) produced using the same process (Fig. 11e). At a current density of 1.25 mA cm^{-2}, the asymmetric device maintained 92 % of its initial capacitance following a 10,000 cycle long-term stability test [130].

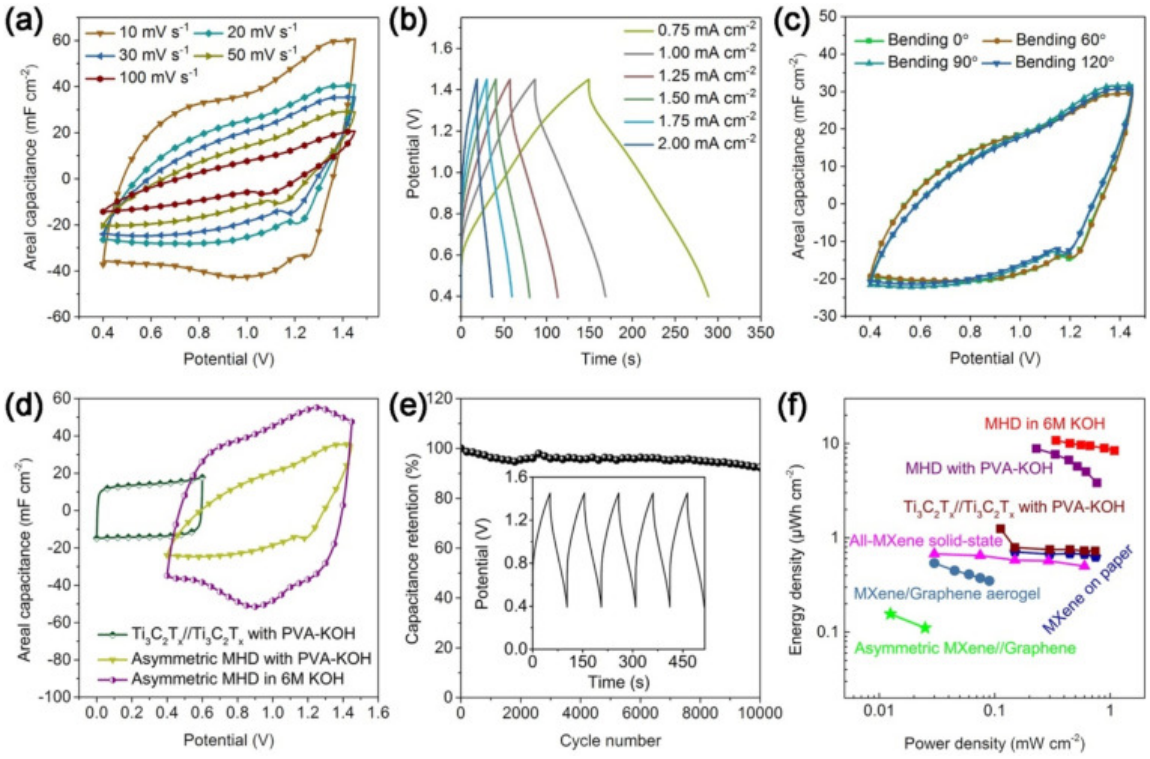

Fig. 11. CV curves of asymmetric MHDs at various scan rates. (b) GCD curves at various current densities. (c) CV curves obtained at various bending angles at 30 mV s^{-1}. (d) Comparison of CV curves in 6 M KOH electrolyte at 30 mV s^{-1}. (e) The cycle performance of the device (the final five charge-discharge cycles at 1.25 mA cm^{-2} are included in the inset) (f) Ragone plots of the microsupercapacitors as compared with the literature [130].

Fan et al. have also reported the use of CNTs/MnO_2 battery-type electrodes in conjunction with MXene/TOBC@PPy capacitor-type electrodes to prepare a unique zinc-ion hybrid micro-supercapacitor (ZHMSC) as shown in Fig. 12 [131]. By boosting the ionic and electronic transport between the MXene interlayers, this synthesis approach raises the energy density to a level comparable to the MB device. As the scan rate is increased from 2 to 6 mV s^{-1}, the capacitive effect contribution ratio progressively rises from 44.7 % to 59.4 %. The optimized MXene/BC@PPy capacitor-type electrode and the asymmetric electrode design allowed for the creation of ZHMSCs that demonstrated a high areal energy density of 145.4 μWh cm^{-2} and an excellent retention (95.8 %) after 25,000 cycles, which was on par with micro-batteries. Furthermore, even during 400 % elongation in tensile deformation, ZHMSCs can be guaranteed to produce stable energy production. The exceptional stretchability was credited to the use of the innovative liquid-metal-island-bridge architecture, which brought together the mechanically malleable structure and the intrinsically stretchable liquid-metal circuit with a high electric stress endurance. A summary of the MXene ternary composites used in micro-supercapacitors is displayed in Table 2.

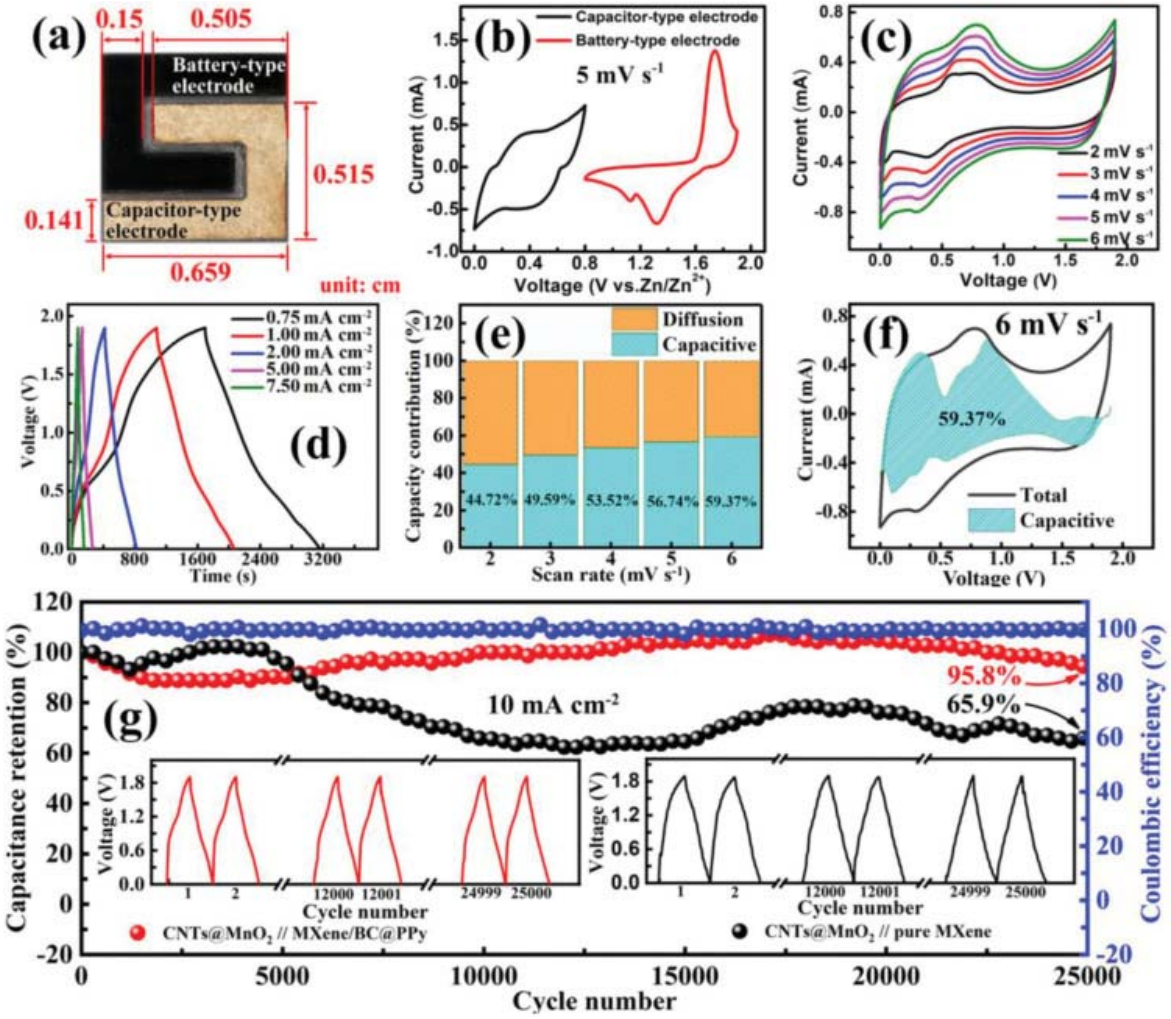

Fig. 12. Representative photograph of a ZHMSC unit assembled based on MXene/BC@PPy capacitor-type electrode and CNTs@MnO_2 battery-type electrode; b) CV curves of the MXene/BC@PPy capacitor-type electrode and CNTs@MnO_2 battery-type electrode; c) CV curves of the ZHMSC at various scan rates; d) GCD curves at different current densities; e) Pseudocapacitive contributions of MXene/BC@PPy capacitor-type electrode at various scan rates; f) CV curve at 6 mV s^{-1} with a marked region representing the capacitive controlled contribution of about 59.37 %; g) Cycling stability test of the ZHMSC based on MXene/BC@PPy and pure MXene capacitor-type electrodes with the same CNTs@MnO_2 battery-type electrode [131].

Table 2. MXene ternary composites for microsupercapacitors.

Devices based on ternary MXene	Capacitance	Energy density	Power density	Capacitance retention	Ref.
CNTs/MXene–TPU hybrid fibers	3.9 F cm^{-3}	1.16 mWh cm^{-3}	0.16 Wcm^{-3}	80/50 cycles	[132]
MXene/BC@PPy	200.47 mF cm^{-2}		0.01 mWh cm^{-2}	82/5000 cycles	[133]
MXene/PEDOT:PSS fibers	614.5 F·cm^{-3}	7.13 Wh cm^{-3}	8249 mWh cm^{-3}	96/200 cycles	[134]
MXene/BC@PPy hybrid film	232.79 mF cm^{-2}	45.3 μWh cm^{-2}		95/5000 cycles	[135]
RGO/CNFs/Ti_3C_2	148.25 F cm^{-3}	20.5 mW h cm^{-3}	0.25 W cm^{-}	93/6000 cycles	[108]
r-GO/MnO_2/Ag NW-PET	2.72 Fcm^{-3}	162.0 mW. cm^{-3}	2.3 mWh. cm^{-3}	90/6000 cycles	[136]
	1632 F/cm^3 at 10 mV s^{-1}	50.6 Wh/L	127 kW/L		
MXene/RuO_2/Ag-NW	864.2 F/cm^3, *v*: 1 mV s^{-1}	13.5 mWh/cm^3	48.5 W/cm^3	90/10,000 cycles	[129]
MXene@TOBC@PPy	388 mF cm^{-2}	145.4 μWh cm^{-2}	3.78	95/25000 cycles	[131]

8. Prospects and challenges

Although MXene-based ternary nanocomposites have made tremendous strides in the last few years in the field of supercapacitor applications, the pertinent research in this realm is still in its early stages. Therefore, it is critical to identify the obstacles that must be overcome to further push the boundaries of research in this area.

i. Most of the present research on MXene ternary composites focuses on how to modify MXene; however, it ignores the comparison of how various materials and MXene types interact to influence the properties of MXene ternary composites. Thus, more studies and comparison of the MXene ternary composites is needed. Improved properties of each individual component that makes up the composites are necessary to achieve high performing composites and ensure useful integration of relevant benefits. This calls for overall improvements in the ternary composites, not just in terms of porosity, optical characteristics, electrical conductivity, large specific area, etc., but also in forms of surface functionalization, reproducibility, and commercialization.

ii. MXenes have low crystallinity and are readily oxidized in the test conditions. Clarifying the structural changes and electrochemical reaction mechanism of MXenes ternary electrodes during different cycles is therefore essential. The charge storage processes of MXene-based ternary nanocomposites electrodes during the electrochemical reaction can be studied by employing in-situ XRD, TEM, and Raman methods. It is crucial to investigate the interfacial processes that occur during the reaction phase and the charge storage mechanisms of MXene-based nanocomposites.

iii. The design of the device and the characteristics of the electrode material govern supercapacitor performance. Scholars are examining various device designs,

like asymmetric supercapacitors and hybrid devices, to enhance the performance of Mxene-based nanocomposites in supercapacitors.

iv. The distribution of MXene nanosheets within the composite material directly affects the characteristics of MXene/composites. To fulfill the necessary parameters, it is therefore essential to achieve a homogenous preparation of MXene/composite with various architectures using appropriate techniques. The genuine interaction mechanism between MXene and other materials in a composite is crucial to understanding and expanding upon. To further understand the improved supercapacitive behavior of MXene ternary composites for SCs, it is imperative to carefully examine the connection between the corresponding surface functional groups and the physical-chemical characteristics of the MXene/cellulose composite.

v. Even though MXenes and MXenes have proven to be exceptionally effective in a range of applications, especially in electrochemistry, more research is still needed to understand the fundamental principles underlying these occurrences. It is probable that MXene sheets' restacking propensity may not be enough to achieve optimal electrochemical performance. The development of commercially available devices based on the materials may be adversely affected by this problem.

vi. Achieving greater quality and dimensional homogeneity in the large-scale manufacturing of MXene-ternary composites for supercapacitors still presents difficult challenges. Successful industrial applications require addressing these issues.

9. Conclusions

MXene, a two-dimensional material with high conductivity, surface functional groups, and intercalation capacitance properties, is promising for modifying supercapacitor electrode composition due to its potential to change electrode composition and advance supercapacitor technology. The electrical, mechanical, and electrochemical charge storage capabilities can be enhanced by modifying their surface chemistry; as a result, these materials are well suited for further investigation in supercapacitors. The developments in MXene-based nanocomposites for supercapacitor applications were mostly covered in this review. Additionally, charge storage mechanisms of MXenes stores in supercapacitor devices are also highlighted. The advantages of mixing MXene material with traditional active ingredients such metal sulfides, metal oxides, conductive polymers, and carbon-based compounds are discussed. The most recent advancements in those MXene-based nanocomposites and their uses in supercapacitors are presented in detail. We conclude that:

i. Ternary MXene composites can be prepared by different methods including vacuum infiltration, solvent-assisted self-assembly, hydrothermal, ultrasonication, electrospinning, among others. However, the synthesis technique adopted influence the surface functional groups, sheet size and interlayer, and ultimately, the electrochemical performance.

ii. Synthesis of ternary MXene composites prevents MXene materials from restacking, and allows the active surface area accessible to ions, leading to superior electrochemical performances.

iii. The MXene-carbon/conducting polymer ternary composites have demonstrated superior electrochemical performance when compared with that of the pristine MXene and carbon/conducting polymer composite. The highly conductive two-

dimensional MXene nanosheets with good electrical contact and the carbon/conducting polymer composite material together form an efficient conductive network, which provides sufficient electron supply for the Faradaic reaction of PANI.

iv. A ternary composite of transition metal sulfide and oxide with MXene shows improved energy density than metal-oxide/MXene binary composites and pure MXenes. This enhancement is due to high theoretical capacitance of transition metal sulfides as compared to metal oxide.

v. The incorporation of metal oxide into the ternary composite resulted in an improvement in its specific capacitance and energy density by creating a larger potential window. Comparing a binary composite electrode to a ternary composite electrode, the latter provided almost twice as much specific capacitance. Because of its improved conductivity and intercalative pseudocapacitive charge storage, the ternary composite demonstrated superior electrochemical performance.

vi. The remarkable electrochemical stability of ternary MXene and MOF composites is key to delivering high hybrid supercapacitor performance since it guarantees steady performance under a variety of operating situations and increases the device's lifespan. This stability is essential to sustaining capacitance and efficiency throughout multiple cycles of charge and discharge.

vii. The use of ternary composites in sophisticated microsupercapacitors with high energy and power densities has also demonstrated considerable promise. This was made possible by the strong pseudocapacitance, metallic conductivity, and simplicity in solution processing of MXenes with other flexible materials.

To sum up, ternary composites based on MXene have advanced tremendously and have a lot of potential applications in supercapacitors. The importance of research in pairing MXene with other potential materials is still quite high. Because of its comprehensive performance, flexible MXene-based composites are expected to become the next generation of supercapacitor electrode materials for advanced energy storage applications. Understanding surface chemistry, designing distinctive structures that support high-performance supercapacitors, and comprehending their capacitive energy storage process will all be crucial in this regard.

CRediT authorship contribution statement

Kabir O. Otun: Writing – review & editing, Writing – original draft, Visualization, Methodology, Investigation, Formal analysis, Data curation, Conceptualization. **Azfarizal Mukhtar:** Writing – review & editing, Writing – original draft, Visualization, Validation, Supervision, Methodology. **Ismail Hossain:** Writing – review & editing, Writing – original draft, Visualization, Resources. **Jibril Abdulsalam:** Writing – review & editing, Writing – original draft, Visualization, Validation.

Declaration of competing interest

The authors declare that they have no known competing financial interests or personal relationships that could have appeared to influence the work reported in this paper.

Acknowledgements

The authors gratefully acknowledge the support of the Universiti Tenaga Malaysia (UNITEN), the Institute of Materials Science, Technical University of Darmstadt 64287 Darmastadt, Germany and the Ministry of Science and Higher Education of the Russian Federation (Ural Federal University Program of Development within the Priority-2030 Program).

Data availability

No data was used for the research described in the article.

References

[1] R. York, S.E. Bell, Energy transitions or additions? Why a transition from fossil fuels requires more than the growth of renewable energy, Energy Res Soc Sci 51 (2019) 40–43, https://doi.org/10.1016/J.ERSS.2019.01.008.

[2] V. Ediger, An integrated review and analysis of multi-energy transition from fossil fuels to renewables, Energy Procedia 156 (2019) 2–6, https://doi.org/10.1016/J.EGYPRO.2018.11.073.

[3] J. Libich, J. Máca, J. Vondrák, O. Čech, M. Sedlaříková, Supercapacitors: properties and applications, J Energy Storage 17 (2018) 224–227, https://doi.org/10.1016/J.EST.2018.03.012.

[4] T. Kim, W. Song, D.Y. Son, L.K. Ono, Y. Qi, Lithium-ion batteries: outlook on present, future, and hybridized technologies, J Mater Chem A Mater 7 (2019) 2942–2964, https://doi.org/10.1039/C8TA10513H.

[5] A. González, E. Goikolea, J.A. Barrena, R. Mysyk, Review on supercapacitors: technologies and materials, Renew. Sustain. Energy Rev. 58 (2016) 1189–1206, https://doi.org/10.1016/J.RSER.2015.12.249.

[6] W. Guo, C. Yu, S. Li, J. Qiu, Toward commercial-level mass-loading electrodes for supercapacitors: opportunities, challenges and perspectives, Energy Environ Sci 14 (2021) 576–601, https://doi.org/10.1039/D0EE02649B.

[7] D.C. Pawar, D.B. Malavekar, A.C. Lokhande, C.D. Lokhande, Facile synthesis of layered reduced graphene oxide/polyaniline (rGO/PANI) composite electrode for flexible asymmetric solid-state supercapacitor, J Energy Storage 79 (2024) 110154, https://doi.org/10.1016/J.EST.2023.110154.

[8] S. Zong, J. Du, A. Chen, X. Gao, K.O. Otun, X. Liu, L.L. Jewell, N-doped crumpled carbon nanotubes as advanced electrode material for supercapacitor, J. Alloys Compd. 928 (2022) 167222, https://doi.org/10.1016/J.JALLCOM.2022.167222.

[9] M. Naguib, M. Kurtoglu, V. Presser, J. Lu, J. Niu, M. Heon, L. Hultman, Y. Gogotsi, M.W. Barsoum, Two-dimensional nanocrystals produced by exfoliation of Ti3AlC2, Adv. Mater. 23 (2011) 4248–4253, https://doi.org/10.1002/ADMA.201102306.

[10] S. Panda, K. Deshmukh, S.K. Khadheer Pasha, J. Theerthagiri, S. Manickam, M. Y. Choi, MXene based emerging materials for supercapacitor applications: recent advances, challenges, and future perspectives, Coord. Chem. Rev. 462 (2022) 214518, https://doi.org/10.1016/J.CCR.2022.214518.

[11] M.W. Barsoum, T. El-Raghy, The MAX phases: unique new carbide and nitride materials: tertiary ceramics are soft and machinable, yet heat-tolerant, strong and lightweight, Am. Sci. 89 (2001) 334–343, https://doi.org/10.1511/2001.4.334.

[12] M.Q. Zhao, C.E. Ren, Z. Ling, M.R. Lukatskaya, C. Zhang, K.L. Van Aken, M. W. Barsoum, Y. Gogotsi, Flexible MXene/carbon nanotube composite paper with high volumetric capacitance, Adv. Mat. 27 (2015) 339–345, https://doi.org/10.1002/ADMA.201404140.

[13] E. Kayali, A. Vahidmohammadi, J. Orangi, M. Beidaghi, Controlling the dimensions of 2D MXenes for ultrahigh-rate pseudocapacitive energy storage, ACS Appl. Mater. Interfaces 10 (2018) 25949–25954, https://doi.org/10.1021/ACSAMI.8B07397.

[14] C. Dai, Y. Chen, X. Jing, L. Xiang, D. Yang, H. Lin, Z. Liu, X. Han, R. Wu, Two-dimensional tantalum carbide (MXenes) composite nanosheets for multiple imaging-guided photothermal tumor ablation, ACS Nano 11 (2017) 12696–12712, https://doi.org/10.1021/ACSNANO.7B07241.

[15] S.Y. Lin, X. Zhang, Two-dimensional titanium carbide electrode with large mass loading for supercapacitor, J. Power Sources 294 (2015) 354–359, https://doi.org/10.1016/j.jpowsour.2015.06.082.

[16] Y. Zhou, K. Luo, X. Zha, Z. Liu, X. Bai, Q. Huang, Z. Guo, C. Te Lin, S. Du, Electronic and transport properties of Ti2CO2 MXene nanoribbons, J. Phys. Chem. C 120 (2016) 17143–17152, https://doi.org/10.1021/ACS.JPCC.6B06426.

[17] E. Pomerantseva, Y. Gogotsi, Two-dimensional heterostructures for energy storage, Nat. Energy 2 (2017) 1–6, https://doi.org/10.1038/NENERGY.2017.89.

[18] R. Mantovani Ronchi, J. Teodoro Arantes, S. Ferreira Santos, Synthesis, Structure, Properties and Applications of MXenes: Current Status and Perspectives, 2019, pp. 18167–18188, https://doi.org/10.1016/j.ceramint.2019.06.114.

[19] Z. Nezafat, A. Mirzaei, M. Nasrollahzadeh, S. Javanshir, Recent advances in MXene-based composite materials with conducting polymers for supercapacitors, J Energy Storage 86 (2024) 111215, https://doi.org/10.1016/j.est.2024.111215.

[20] J. Yang, W. Bao, P. Jaumaux, S. Zhang, C. Wang, G. Wang, J. Yang, S. Zhang, C. Wang, W. Bao, P. Jaumaux, G. Wang, MXene-based composites: synthesis and applications in rechargeable batteries and supercapacitors, Adv. Mater. Interfaces 6 (2019) 1802004, https://doi.org/10.1002/ADMI.201802004.

[21] M. Vijayakumar, G. Elsa, A. Nirogi, R. Navaneethan, A.B. Sankar, M. Karthik, MXenes and their composites for hybrid capacitors and supercapacitors: a critical review, Emerg. Mater. 4 (2021) 655–672, https://doi.org/10.1007/S42247-021-00204-7/FIGURES/16.

[22] S. Jiang, L. Lu, Y. Song, Recent advances of flexible Mxene and its composites for supercapacitors, Chemistry – A European Journal 30 (2024) 202304036, https://doi.org/10.1002/CHEM.202304036.

[23] F. Wang, X. Wu, X. Yuan, Z. Liu, Y. Zhang, L. Fu, Y. Zhu, Q. Zhou, Y. Wu, W. Huang, Latest advances in supercapacitors: from new electrode materials to novel device designs, Chem. Soc. Rev. 46 (2017) 6816, https://doi.org/10.1039/c7cs00205j.

[24] W. Raza, F. Ali, N. Raza, Y. Luo, K.H. Kim, J. Yang, S. Kumar, A. Mehmood, E. E. Kwon, Recent advancements in supercapacitor technology, Nano Energy 52 (2018) 441, https://doi.org/10.1016/j.nanoen.2018.08.013.

[25] Y. Liu, Q. Wu, L. Liu, P. Manasa, L. Kang, F. Ran, Vanadium nitride for aqueous supercapacitors: a topic review, J Mater Chem A Mater 8 (2020) 8218–8233, https://doi.org/10.1039/D0TA01490G.

[26] P. Sharma, V. Kumar, Current technology of supercapacitors: a review, J. Electron. Mater. 49 (2020) 3520–3532, https://doi.org/10.1007/S11664-020-07992-4/METRICS.

[27] K.O. Otun, A. Mukhtar, S.A. Nafiu, I.T. Bello, J. Abdulsalam, Incorporation of redox-activity into metal-organic frameworks for enhanced supercapacitors: a review, J Energy Storage 84 (2024) 110673, https://doi.org/10.1016/J.EST.2024.110673.

[28] A.G. Pandolfo, A.F. Hollenkamp, Carbon properties and their role in supercapacitors, J. Power Sources 157 (2006) 11–27, https://doi.org/10.1016/J.JPOWSOUR.2006.02.065.

[29] J. Balamurugan, T. Tuan Nguyen, V. Aravindan, N. Hoon Kim, J. Hee Lee, J. Balamurugan, T.T. Nguyen, N.H. Kim, J.H. Lee, V. Aravindan, Flexible solid-state asymmetric supercapacitors based on nitrogen-doped graphene encapsulated ternary metal-nitrides with ultralong cycle life, Adv. Funct. Mater. 28 (2018) 1804663, https://doi.org/10.1002/ADFM.201804663.

[30] J. Balamurugan, P.M. Austeria, J.B. Kim, E.S. Jeong, H.H. Huang, D.H. Kim, N. Koratkar, S.O. Kim, Electrocatalysts for zinc–air batteries featuring single molybdenum atoms in a nitrogen-doped carbon framework, Adv. Mater. 35 (2023) 2302625, https://doi.org/10.1002/ADMA.202302625.

[31] A. González, E. Goikolea, J.A. Barrena, R. Mysyk, Review on supercapacitors: technologies and materials, Renew. Sustain. Energy Rev. 58 (2016) 1189–1206, https://doi.org/10.1016/J.RSER.2015.12.249.

[32] M. Naguib, M. Kurtoglu, V. Presser, J. Lu, J. Niu, M. Heon, L. Hultman, Y. Gogotsi, M.W. Barsoum, Two-dimensional nanocrystals produced by exfoliation of Ti3AlC2, Adv. Mater. 23 (2011) 4248–4253, https://doi.org/10.1002/ADMA.201102306.

[33] Y. Liu, J. Yu, D. Guo, Z. Li, Y. Su, Ti3C2Tx MXene/graphene nanocomposites: synthesis and application in electrochemical energy storage, J. Alloys Compd. 815 (2020) 152403, https://doi.org/10.1016/J.JALLCOM.2019.152403.

[34] Y. Abu Dakka, J. Balamurugan, R. Balaji, N.H. Kim, J.H. Lee, Advanced Cu0.5Co0.5Se2 nanosheets and MXene electrodes for high-performance asymmetric supercapacitors, Chem. Eng. J. 385 (2020) 123455, https://doi.org/10.1016/J.CEJ.2019.123455.

[35] A. Choubey, A. Yadav, MXene and transition metal chalcogenides-based 2D nanomaterials for next-generation supercapacitors, J Energy Storage 79 (2024) 110131, https://doi.org/10.1016/J.EST.2023.110131.

[36] J. Balamurugan, C. Li, V. Aravindan, N. Hoon Kim, J. Hee Lee, J. Balamurugan, C. Li, N.H. Kim, J.H. Lee, V. Aravindan, Hierarchical Ni-Mo-S and Ni-Fe-S nanosheets with ultrahigh energy density for flexible all solid-state supercapacitors, Adv. Funct. Mater. 28 (2018) 1803287, https://doi.org/10.1002/ADFM.201803287.

[37] K. Das, D. Majumdar, Prospects of MXenes/graphene nanocomposites for advanced supercapacitor applications, J. Electroanal. Chem. 905 (2022) 115973, https://doi.org/10.1016/J.JELECHEM.2021.115973.

[38] R. Syamsai, A.N. Grace, Ta4C3 MXene as supercapacitor electrodes, J. Alloys Compd. 792 (2019) 1230–1238, https://doi.org/10.1016/J.JALLCOM.2019.04.096.

[39] Y. Wang, Y. Song, Y. Xia, Electrochemical capacitors: mechanism, materials, systems, characterization and applications, Chem. Soc. Rev. 45 (2016) 5925–5950, https://doi.org/10.1039/C5CS00580A.

[40] M. Hu, H. Zhang, T. Hu, B. Fan, X. Wang, Z. Li, Emerging 2D MXenes for supercapacitors: status, challenges and prospects, Chem. Soc. Rev. 49 (2020) 6666–6693, https://doi.org/10.1039/D0CS00175A.

[41] J. Xu, J. You, L. Wang, Z. Wang, H. Zhang, MXenes serving aqueous supercapacitors: preparation, energy storage mechanism and electrochemical performance enhancement, Sustain. Mater. Technol. 33 (2022) e00490, https://doi.org/10.1016/J.SUSMAT.2022.E00490.

[42] R. Mohanty, A. Nashim, K. Parida, K. Parida, Can doped-Mxene-based supercapacitors be the game-changer for future energy landscape? A critical perspective, Langmuir 40 (2024) 14197–14213, https://doi.org/10.1021/ACS.LANGMUIR.4C01242/ASSET/IMAGES/LARGE/LA4C01242_0004.JPEG.

[43] R. Ibragimova, P. Erhart, P. Rinke, H.P. Komsa, Surface functionalization of 2D Mxenes: trends in distribution, composition, and electronic properties, J. Phys. Chem. Lett. 12 (2021) 2377–2384, https://doi.org/10.1021/ACS.JPCLETT.0C03710/ASSET/IMAGES/LARGE/JZ0C03710_0006.JPEG.

[44] M. Rostami, A. Badiei, G.M. Ziarani, J. Azadmanjiri, Unlocking the power of nano-heterostructured engineering: advancements in Ti3C2Tx MXene-based heterojunctions for rechargeable ion batteries, J Energy Storage 82 (2024) 110583, https://doi.org/10.1016/J.EST.2024.110583.

[45] P. Baraneedharan, D. Shankari, A. Arulraj, Nanotechnology synthesis and applications of MXene-based composites: a review in nanoengineering of mxene-based field-effect transistor gas sensors: advancements in next-generation electronic devices, J. Electrochem. Soc. (2023) 107501, https://doi.org/10.1088/1361-6528/acc7a8.

[46] M. Rostami, A. Badiei, G.M. Ziarani, A review of recent progress in the synthesis of 2D Ti3C2Tx MXenes and their multifunctional applications, Inorg. Chem. Commun. 163 (2024) 112362, https://doi.org/10.1016/J.INOCHE.2024.112362.

[47] M.R. Lukatskaya, O. Mashtalir, C.E. Ren, Y. Dall'Agnese, P. Rozier, P.L. Taberna, M. Naguib, P. Simon, M.W. Barsoum, Y. Gogotsi, Cation intercalation and high volumetric capacitance of two-dimensional titanium carbide, Science 341 (2013) (1979) 1502–1505, https://doi.org/10.1126/SCIENCE.1241488.

[48] V. Bayram, M. Ghidiu, J.J. Byun, S.D. Rawson, P. Yang, S.A. McDonald, M. Lindley, S. Fairclough, S.J. Haigh, P.J. Withers, M.W. Barsoum, I.A. Kinloch, S. Barg, MXene tunable lamellae architectures for supercapacitor electrodes, ACS Appl Energy Mater 3 (2020) 411–422, https://doi.org/10.1021/ACSAEM.9B01654.

[49] N. He, S. Patil, J. Qu, J. Liao, F. Zhao, W. Gao, Effects of electrolyte mediation and mxene size in fiber-shaped supercapacitors, ACS Appl Energy Mater 3 (2020) 2949–2958, https://doi.org/10.1021/ACSAEM.0C00024/ASSET/IMAGES/LARGE/AE0C00024_0005.JPEG.

[50] E. Kayali, A. Vahidmohammadi, J. Orangi, M. Beidaghi, Controlling the dimensions of 2D Mxenes for ultrahigh-rate pseudocapacitive energy storage, acs appl mater interfaces 10 (2018) 25949–25954, https://doi.org/10.1021/ACSAMI.8B07397/ASSET/IMAGES/LARGE/AM-2018-07397D_0004.JPEG.

[51] M. Gao, F. Wang, S. Yang, A. Gaetano Ricciardulli, F. Yu, J. Li, J. Sun, R. Wang, Y. Huang, P. Zhang, X. Lu, Engineered 2D MXene-based materials for advanced supercapacitors and micro-supercapacitors, Mater. Today 72 (2024) 318–358, https://doi.org/10.1016/J.MATTOD.2023.12.009.

[52] N.A. Althubiti, S. Aman, T.A.M. Taha, Synthesis of MnFe2O4/MXene/NF nanosized composite for supercapacitor application, Ceram. Int. 49 (2023) 27496–27505, https://doi.org/10.1016/J.CERAMINT.2023.06.025.

[53] A. Sugahara, Y. Ando, S. Kajiyama, K. Yazawa, K. Gotoh, M. Otani, M. Okubo, Yamada, Negative dielectric constant of water confined in nanosheets, Nat. Commun. (2019) 850, https://doi.org/10.1038/s41467-019-08789-8.

[54] H. Shao, Z. Lin, K. Xu, P.L. Taberna, P. Simon, Electrochemical study of pseudocapacitive behavior of Ti3C2Tx MXene material in aqueous electrolytes, Energy Storage Mater 18 (2019) 456–461, https://doi.org/10.1016/J.ENSM.2018.12.017.

[55] C. Yang, Y. Tang, Y. Tian, Y. Luo, M. Faraz Ud Din, X. Yin, W. Que, C. Yang, Y. Tang, Y. Tian, Y. Luo, M. Faraz Ud Din, X. Yin, W. Que, Flexible nitrogen-doped 2d titanium carbides (mxene) films constructed by an ex situ solvothermal method with extraordinary volumetric capacitance, Adv Energy Mater 8 (2018) 1802087, https://doi.org/10.1002/AENM.201802087.[56] M. Rostami, A. Badiei, Molten salt-shielded preparation of the ultrathin nanosheets of Ti3C2Cl2 @TiO2 coupled with Fe3O4@C-C3N4 for assessing photocatalytic activity, Ceram. Int. 50 (2024) 13608–13620, https://doi.org/10.1016/J.CERAMINT.2024.01.275.

[57] C. Xu, W.Y. Jiang, L. Guo, M. Shen, B. Li, J.Q. Wang, High supercapacitance performance of nitrogen-doped Ti3C2Tx prepared by molten salt thermal treatment, Electrochim. Acta 403 (2022) 139528, https://doi.org/10.1016/J.ELECTACTA.2021.139528.

[58] J. Zhu, Y. Tang, C. Yang, F. Wang, M. Cao, Composites of TiO2 nanoparticles deposited on ti3c2 mxene nanosheets with enhanced electrochemical performance, J. Electrochem. Soc. 163 (2016) A785–A791, https://doi.org/10.1149/2.0981605JES.

[59] M. Rostami, P. Rezvaninia, A. Amiri, G. Mohammadi Ziarani, M.R. Ganjali, Badiei, Hybrid nano-architectural engineering of Ti3C2Tx MXene heterostructures for supercapacitor applications: a review, Results in Engineering 22 (2024) 102227, https://doi.org/10.1016/J.RINENG.2024.102227.

[60] W. Ding, L. Hu, J. Dai, X. Tang, R. Wei, Z. Sheng, C. Liang, D. Shao, W. Song, Q. Liu, M. Chen, X. Zhu, S. Chou, X. Zhu, Q. Chen, Y. Sun, S.X. Dou, Highly ambient-stable 1t-mos2 and 1t-ws2 by hydrothermal synthesis under high magnetic fields, ACS Nano 13 (2019) 1694–1702, https://doi.org/10.1021/ACSNANO.8B07744/ASSET/IMAGES/LARGE/NN-2018-07744N_0005.JPEG.

[61] Q.X. Xia, N.M. Shinde, T. Zhang, J.M. Yun, A. Zhou, R.S. Mane, S. Mathur, K. H. Kim, Seawater electrolyte-mediated high volumetric MXene-based electrochemical symmetric supercapacitors, Dalton Trans. 47 (2018) 8676–8682, https://doi.org/10.1039/C8DT01375F.

[62] H. He, J. Wang, Q. Xia, L. Wang, Q. Hu, A. Zhou, Effect of electrolyte on supercapacitor performance of two-dimensional molybdenum carbide (Mo2CTx) MXene prepared by hydrothermal etching, Appl. Surf. Sci. 568 (2021) 150971, https://doi.org/10.1016/J.APSUSC.2021.150971.

[63] N. He, S. Patil, J. Qu, J. Liao, F. Zhao, W. Gao, Effects of electrolyte mediation and MXene size in fiber-shaped supercapacitors, ACS Appl Energy Mater 3 (2020) 2949–2958, https://doi.org/10.1021/ACSAEM.0C00024/ASSET/IMAGES/LARGE/AE0C00024_0005.JPEG.

[64] Z. Lin, D. Barbara, P.L. Taberna, K.L. Van Aken, B. Anasori, Y. Gogotsi, P. Simon, Capacitance of Ti3C2Tx MXene in ionic liquid electrolyte, J. Power Sources 326 (2016) 575–579, https://doi.org/10.1016/J.JPOWSOUR.2016.04.035.

[65] K. Nasrin, K. Subramani, M. Karnan, M. Sathish, MnCo2S4 – MXene: a novel hybrid electrode material for high performance long-life asymmetric supercapattery, J. Colloid Interface Sci. 600 (2021) 264–277, https://doi.org/10.1016/J.JCIS.2021.05.037.

[66] S.A. Beknalkar, A.M. Teli, A.C. Khot, S.M. Mane, J.C. Shin, Preparation of CuMn2O4/Ti3C2 MXene composite electrodes for supercapacitors with high energy density and study on their charge transfer kinetics, Ceram. Int. 49 (2023) 31236–31247, https://doi.org/10.1016/J.CERAMINT.2023.07.071.

[67] A. Patra, K. Pramoda, S. Hegde, B. Chakraborty, C.S. Rout, All-solid-state flexible supercapacitor based on a binary transition metal dichalcogenide grown on 2D/2D heterostructure materials, J Energy Storage 68 (2023) 107825, https://doi.org/10.1016/j.est.2023.107825.

[68] A. Raveendran, M. Chandran, M.R. Siddiqui, S.M. Wabaidur, S. Angaiah, R. Dhanusuraman, Binary Ni-Cu Nanocomposite-modified MXene-adorned 3D-nickel Foam for Effective Overall Water Splitting and Supercapacitor Applications, 2024, pp. 1509–1525, https://doi.org/10.1039/d4se00058g.

[69] J. Kim, J.H. Ryu, M. Jang, S. Park, M. Kim, K.H. Lee, S. Choi, Y. Yoon, H.K. Jung, S.S. Lee, K.S. An, One-dimensional π-d conjugated coordination polymer intercalated MXene compound for high-performance supercapacitor electrode, Small Methods 7 (2023) 2201539, https://doi.org/10.1002/SMTD.202201539.

[70] S. Xu, Y. Li, T. Mo, G. Wei, Y. Yang, Highly matched porous MXene anodes and graphene cathodes for high-performance aqueous asymmetric supercapacitors, Energy Storage Mater 69 (2024) 103379, https://doi.org/10.1016/J.ENSM.2024.103379.

[71] D. Parajuli, N. Murali, D.K. C, B. Karki, K. Samatha, A.A. Kim, M. Park, B. Pant, Advancements in Mxene-polymer nanocomposites in energy storage and biomedical applications, Polymers 14 (2022) 3433, https://doi.org/10.3390/POLYM14163433, 2022, Vol. 14, Page 3433.[72] S. Cho, J. Lim, Y. Seo, Flexible solid supercapacitors of novel nanostructured electrodes outperform most supercapacitors, ACS Omega 7 (2022) 37825–37833, https://doi.org/10.1021/ACSOMEGA.2C04822/ASSET/IMAGES/LARGE/AO2C04822_0005.JPEG.

[73] L. Yang, W. Zheng, P. Zhang, J. Chen, W.B. Tian, Y.M. Zhang, Z.M. Sun, MXene/CNTs films prepared by electrophoretic deposition for supercapacitor electrodes, J. Electroanal. Chem. (2018) 1–6, https://doi.org/10.1016/j.jelechem.2018.10.024.

[74] M.N. Mustafa, M.A.A. Mohd Abdah, N. Mohamad Saidi, W.P. Wong, Y.S. Tan, Numan, Y. Sulaiman, R. Walvekar, F.N. Mohammad Azlan, M. Khalid, High-performance electrochromic supercapacitor with bimetallic phosphate and vanadium carbide MXene, J. Power Sources 595 (2024) 234079, https://doi.org/10.1016/J.JPOWSOUR.2024.234079.

[75] Z. Fan, Y. Wang, Z. Xie, D. Wang, Y. Yuan, H. Kang, B. Su, Z. Cheng, Y. Liu, Z. Fan, D. Wang, Y. Yuan, H. Kang, Y. Liu, Y. Wang, Z. Xie, B. Su, Z. Cheng, Modified MXene/holey graphene films for advanced supercapacitor electrodes with superior energy storage, Adv. Sci. 5 (2018) 1800750, https://doi.org/10.1002/ADVS.201800750.

[76] M.Q. Zhao, C.E. Ren, Z. Ling, M.R. Lukatskaya, C. Zhang, K.L. Van Aken, M. W. Barsoum, Y. Gogotsi, Flexible MXene/carbon nanotube composite paper with high volumetric capacitance, Adv. Mater. 27 (2015) 339–345, https://doi.org/10.1002/ADMA.201404140.

[77] M. Pathak, B. Chakraborty, C.S. Rout, Facile in-situ grown spinel MnCo2O4/MWCNT and MnCo2O4/Ti3C2 MXene composites for high-performance asymmetric supercapacitor with theoretical insight, J Energy Storage 66 (2023) 107475, https://doi.org/10.1016/j.est.2023.107475.

[78] W. Luo, Y. Wei, Z. Zhuang, Z. Lin, X. Li, C. Hou, T. Li, Y. Ma, Fabrication of Ti3C2Tx MXene/polyaniline composite films with adjustable thickness for high-performance flexible all-solid-state symmetric supercapacitors, Electrochim. Acta 406 (2022) 139871, https://doi.org/10.1016/j.electacta.2022.139871.

[79] H.S. Nishad, S.M. Mane, S.P. Patole, J. Lee, S. Gosavi, P.S. Walke, Temperature driven pseudocapactive performance of WO3/MXene nanocomposite for asymmetric aqueous supercapacitors, Chem. Eng. J. 495 (2024) 153360, https://doi.org/10.1016/J.CEJ.2024.153360.

[80] W. Luo, Y. Wei, Z. Zhuang, Z. Lin, X. Li, C. Hou, T. Li, Y. Ma, Fabrication of Ti3C2Tx MXene/polyaniline composite films with adjustable thickness for high-performance flexible all-solid-state symmetric supercapacitors, Electrochim. Acta 406 (2022) 139871, https://doi.org/10.1016/j.electacta.2022.139871.

[81] S.S. Dongre, A. Iqbal, R. Thapa, S. Ramu, R. Geetha Balakrishna, Synergistic catalyst design for enhanced electrochemical hydrogen evolution: Fe2O3/MoS2/Ti3C2Tx MXene ternary composite, ACS Appl. Eng. Mater 2024 (2024) 943–954, https://doi.org/10.1021/acsaenm.4c00027.

[82] Y. Cai, W. Zhang, J. Zhao, Y. Wang, Flexible structural construction of the ternary composite Ni,Co-Prussian blue analogue@MXene/polypyrrole for high-capacity capacitive deionization, Appl. Surf. Sci. (2023) 156926, https://doi.org/10.1016/j.apsusc.2023.156926.

[83] Y.Z. Cai, Y.S. Fang, W.Q. Cao, P. He, M.S. Cao, MXene-CNT/PANI ternary material with excellent supercapacitive performance driven by synergy, J. Alloys Compd. 868 (2021) 159159, https://doi.org/10.1016/J.JALLCOM.2021.159159.

[84] Y. Wang, N. Chen, Y. Liu, X. Zhou, B. Pu, Y. Qing, M. Zhang, X. Jiang, J. Huang, Q. Tang, B. Zhou, W. Yang, MXene/Graphdiyne nanotube composite films for free-standing and flexible solid-state supercapacitor, Chem. Eng. J. 450 (2022) 138398, https://doi.org/10.1016/J.CEJ.2022.138398.

[85] L. Cheng, Y. Qu, J. Sun, Preparation of CF@MXene/PANI fiber electrodes for high-performance flexible supercapacitors, J. Mater. Sci. Mater. Electron. (2023) 1–12, https://doi.org/10.1007/S10854-022-09562-2/FIGURES/6.

[86] G. Wang, N. Jiang, Y. Xu, Z. Zhang, G. Wang, K. Cheng, Solvent-assisted assembly of reduced graphene oxide/MXene-polypyrrole composite film for flexible supercapacitors, J. Colloid Interface Sci. 630 (2023) 817–827, https://doi.org/10.1016/J.JCIS.2022.10.135.

[87] J. Vigneshwaran, J. Jose, S. Thomas, A. Gagliardi, R.L. Narayan, S.P. Jose, PPy-PdO modified MXene for flexible binder-free electrodes for asymmetric supercapacitors: insights from experimental and DFT investigations, Chem. Eng. J. 487 (2024) 150555, https://doi.org/10.1016/J.CEJ.2024.150555.

[88] X. Lu, J. Zhu, W. Wu, B. Zhang, Hierarchical architecture of PANI@TiO2/Ti3C2Tx ternary composite electrode for enhanced electrochemical performance, Electrochim. Acta 228 (2017) 282–289, https://doi.org/10.1016/J.ELECTACTA.2017.01.025.

[89] J. Zhou, B.-B. Liu, H. Zheng, W.-Q. Ma, Q. Li, C.-X. Xu, One-step construction of strongly coupled Co3V2O8/Co3O4/MXene heterostructure via in-situ Co-F bonds for high performance all-solid-state asymmetric supercapacitors, Rare Metals (2024) 682–691, https://doi.org/10.1007/s12598.

[90] R.A. Chavan, D.M. Ulisso, A.S. Rasal, J.Y. Chang, A.V. Ghule, Facile synthesis of ternary MXene nanocomposites as an electrode for supercapacitive applications, Mater. Adv (2023) 2659–2666, https://doi.org/10.1039/d3ma00133d.

[91] M.S. Iyer, P. Rajkumar, G. Parvathy, K. Aravinth, J. Kim, Elevating energy storage performance of bismuth antimonate coupled with MXene and graphitic nanofibers in advanced supercapacitors, J. Power Sources 602 (2024) 378–7753, https://doi.org/10.1016/j.jpowsour.2024.234379.

[92] H. Xie, S. Ma, Z. He, Facile preparation of PANI/MoOx nanowires decorated MXene film electrodes for electrochemical supercapacitors, Electrochim. Acta 448 (2023) 142173, https://doi.org/10.1016/J.ELECTACTA.2023.142173.

[93] M. Moniruzzaman, C.K. Maity, S. De, M.J. Kim, J. Kim, SnO2 Nanosphere/carbon dot-embedded ti3c2tx mxene nanocomposites for high-performance binder-free asymmetric supercapacitor electrodes, ACS Appl Nano Mater 7 (2024) 6636–6649, https://doi.org/10.1021/ACSANM.4C00550/ASSET/IMAGES/LARGE/AN4C00550_0007.JPEG.

[94] K. Donthula, R. Araga, N. Thota, S. Sundarrajan, S. Ramakrishna, M. Kakunuri, Hierarchically structured carbon nanofibers with embedded MXene and coated with cobalt oxide as a high-performance electrode for supercapacitors, J Energy Storage 83 (2024) 110686, https://doi.org/10.1016/j.est.2024.110686.

[95] A. Shahid, Z.N. Kayani, S. Riaz, S. Naseem, Enhanced supercapacitor potential of CeO2/MXene nanocomposites with tunable conductive polyaniline concentrations, Diamond Relat. Mater. 146 (2024) 111167, https://doi.org/10.1016/J.DIAMOND.2024.111167.

[96] A. Shahid, Z.N. Kayani, S. Riaz, S. Naseem, Enhanced supercapacitor potential of CeO2/MXene nanocomposites with tunable conductive polyaniline concentrations, Diamond Relat. Mater. 146 (2024) 111167, https://doi.org/10.1016/J.DIAMOND.2024.111167.

[97] S. De, S. Acharya, C. Kumar Maity, G. Chandra Nayak, Boron nitride/Ti3C2Tx Mxene nanosheet/Ws2 nanostructure ternary composites for all-solid-state flexible asymmetric supercapacitors, ACS Appl. Nano Mater 6 (2023) 11175–11186, https://doi.org/10.1021/acsanm.3c01202.

[98] S. Hussain, D. Vikraman, Z. Ali Sheikh, M. Taqi Mehran, F. Shahzad, K. Mujasam Batoo, H.S. Kim, D.K. Kim, M. Ali, J. Jung, WS2-embedded MXene/GO hybrid nanosheets as electrodes for asymmetric supercapacitors and hydrogen evolution reactions, Chem. Eng. J. (2023) 139523, https://doi.org/10.1016/J.CEJ.2022.139523.

[99] A. Sharma, C.S. Rout, 1T metallic vanadium disulfide hybridized with MXene and functionalized-MWCNT as a remarkable electrode for high power density asymmetric supercapacitor applications, Int. J. Energy Res. 46 (2022) 24537–24553, https://doi.org/10.1002/ER.8564.

[100] D.S. Abraham, M. Vinoba, M. Bhagiyalakshmi, NiFe-LDH/MoS2/MXene nanocomposites as an electrode material for battery-type supercapacitors, ACS Appl Nano Mater 7 (2024) 5791–5801, https://doi.org/10.1021/ACSANM.3C03779/ASSET/IMAGES/LARGE/AN3C03779_0008.JPEG.

[101] Y. Liu, J. Gong, J. Wang, C. Hu, M. Xie, X. Jin, S. Wang, Y. Dai, Facile fabrication of MXene supported nickel-cobalt selenide ternary composite via one-step hydrothermal for high-performance asymmetric supercapacitors, J. Alloys Compd. (2021) 163354, https://doi.org/10.1016/j.jallcom.2021.163354.

[102] Y. Yang, X. Huang, C. Sheng, Y. Pan, Y. Huang, X. Wang, In-situ formation of MOFs derivatives CoSe2/Ni3Se4 nanosheets on MXene nanosheets for hybrid supercapacitor with enhanced

electrochemical performance, J. Alloys Compd. (2022) 165908, https://doi.org/10.1016/j.jallcom.2022.165908.

[103] M.S. Javed, X. Zhang, S. Ali, A. Mateen, M. Idrees, M. Sajjad, S. Batool, A. Ahmad, M. Imran, T. Najam, W. Han, Heterostructured bimetallic–sulfide@layered Ti3C2Tx–MXene as a synergistic electrode to realize high-energy-density aqueous hybrid-supercapacitor, Nano Energy 101 (2022) 107624, https://doi.org/10.1016/J.NANOEN.2022.107624.

[104] R. Samal, P. Mane, S. Ratha, B. Chakraborty, C.S. Rout, Rational design of dynamic bimetallic NiCoSe2/2D Ti3C2Tx MXene hybrids for a high-performance flexible supercapacitor and hydrogen evolution reaction, Energy Fuels 36 (2022) 15066–15079, https://doi.org/10.1021/ACS.ENERGYFUELS.2C02808/ASSET/IMAGES/LARGE/EF2C02808_0010.JPEG.

[105] T. Kshetri, D. Khumujam, I. Singh, Y.S. Lee, N.H. Kim, J.H. Lee, Co-MOF@MXene-carbon nanofiber-based freestanding electrodes for a flexible and wearable quasi-solid-state supercapacitor, Chem. Eng. J. 437 (2022) 1385–8947, https://doi.org/10.1016/j.cej.2022.135338.

[106] D.S. Abraham, M. Vinoba, M. Bhagiyalakshmi, NiFe-LDH/MoS2/MXene nanocomposites as an electrode material for battery-type supercapacitors, ACS Appl Nano Mater 7 (2024) 5791–5801, https://doi.org/10.1021/ACSANM.3C03779/ASSET/IMAGES/LARGE/AN3C03779_0008.JPEG.

[107] Y. Liu, H. Zhou, W. Zhou, S. Meng, C. Qi, Z. Liu, T. Kong, Y. Liu, S. Meng, Z. Liu, H. Zhou, W.X. Zhou, T. Kong, C. Qi, Biocompatible, high-performance, wet-adhesive, stretchable all-hydrogel supercapacitor implant based on PANI@rGO/Mxenes electrode and hydrogel electrolyte, Adv Energy Mater 11 (2021) 2101329, https://doi.org/10.1002/AENM.202101329.

[108] J. Wei, Y. Teng, T. Meng, X. Bu, H. Du, D. Li, A multicomponent interconnected composite paper for triple-mode sensors and flexible micro-supercapacitors, J. Mater. Chem. A (2020) 24620–24634, https://doi.org/10.1039/d0ta06775j.

[109] X. Zhou, Y. Qin, X. He, Q. Li, J. Sun, Z. Lei, Z.H. Liu, Ti3C2Tx Nanosheets/Ti3C2Tx quantum dots/rGO (reduced graphene oxide) fibers for an all-solid-state asymmetric supercapacitor with high volume energy density and good flexibility, ACS Appl. Mater. Interfaces 12 (2020) 11833–11842, https://doi.org/10.1021/ACSAMI.9B21874/ASSET/IMAGES/LARGE/AM9B21874_0006.JPEG

[110] H. Tang, R. Chen, Q. Huang, W. Ge, X. Zhang, Y. Yang, X. Wang, Scalable manufacturing of leaf-like MXene/Ag NWs/cellulose composite paper electrode for all-solid-state supercapacitor, EcoMat 4 (2022) e12247, https://doi.org/10.1002/EOM2.12247.

[111] M. Shi, P. Xiao, J. Lang, C. Yan, X. Yan, Porous g-C3N4 and MXene dual-confined FeOOH quantum dots for superior energy storage in an ionic liquid, Adv. Sci. (2020) 1901975, https://doi.org/10.1002/ADVS.201901975.

[112] X. Wu, W. Hu, J. Qiu, B. Geng, M. Du, Q. Zheng, Solvent-assisted self-assembly to fabricate a ternary flexible free-standing polyaniline@MXene-CNTs electrode for high-performance supercapacitors, J. Alloys Compd. (2022) 166062, https://doi.org/10.1016/j.jallcom.2022.166062.

[113] K. Donthula, U.R. Malothu, R. Araga, R. Vooradi, V.S. Patnaikuni, M.V. Reddy, M. Kakunuri, Flexible polyaniline/MXene/CNF composite nanofibrous mats as high-performance supercapacitor electrodes, Polym. Compos. (2023) 7571–7584, https://doi.org/10.1002/PC.27646.

[114] X. Gao, X. Du, T.S. Mathis, M. Zhang, X. Wang, J. Shui, Y. Gogotsi, M. Xu, Maximizing ion accessibility in MXene-knotted carbon nanotube composite electrodes for high-rate electrochemical energy storage, Nat. Commun. (2020) 6160, https://doi.org/10.1038/s41467-020-19992-3.

[115] R. Liu, A. Zhang, J. Ang, J. Ian, W. Huang, J. Cai, C. Barrow, W. Yang, A. Liu, Supercapacitors fabrication of cobaltosic oxide nanoparticle-doped Mxene/graphene hybrid porous aerogels for all-solid-state supercapacitors, Chem. A Eur. J. (2018) 06342, https://doi.org/10.1002/chem.201806342.

[116] T. Arun, A. Mohanty, A. Rosenkranz, B. Wang, J. Yu, M.J. Morel, R. Udayabhaskar, S.A. Hevia, A. Akbari-Fakhrabadi, R.V. Mangalaraja, A. Ramadoss, Role of electrolytes on the electrochemical characteristics of Fe3O4/MXene/RGO composites for supercapacitor applications, Electrochim. Acta 367 (2021) 137473, https://doi.org/10.1016/j.electacta.2020.137473.

[117] J. Chen, Y. Ren, H. Zhang, F. Zhou, J. Qi, Y. Sui, F. Wei, Self-supporting in situ growth Ni3S2/FL-Ti3C2 (MXene)/Ni composite as positive electrode for asymmetrical supercapacitor, J. Mater. Sci. Mater. Electron. 32 (2021) 9721–9729, https://doi.org/10.1007/S10854-021-05633-Y/FIGURES/3.

[118] L. Qin, Q. Tao, A. El Ghazaly, J. Fernandez-Rodriguez, P.O.Å. Persson, J. Rosen, F. Zhang, L. Qin, Q. Tao, A. El-Ghazaly, P.O.Å. Persson, J. Rosen, F. Zhang, J. Fernandez-Rodriguez, High-performance ultrathin flexible solid-state supercapacitors based on solution processable Mo1.33C MXene and PEDOT:PSS, Adv. Funct. Mater. 28 (2018) 1703808, https://doi.org/10.1002/ADFM.201703808.

[119] P. Baraneedharan, D. Shankari, A. Arulraj al, U. Noor, M. Furqan Mughal, T. Ahmed, Binder-free ruthenium oxide/MXene/carbon nanofiber ternary composite electrode for supercapacitors, J. Electrochem. Soc. 170 (2023) 030508, https://doi.org/10.1149/1945-7111/ACBEE5.

[120] M. Moniruzzaman, C. Kumar Maity, S. De, M. Jong Kim, J. Kim, SnO2 Nanosphere/carbon dot-embedded TI3C2TX Mxene nanocomposites for high-performance binder-free asymmetric supercapacitor electrodes, ACS Appl. Nano Mater 7 (2024) 6636–6649, https://doi.org/10.1021/acsanm.4c00550.

[121] Z. Zhao, X. Wu, Z. Zhao, X. Wu, Electrostatic-assembled MXene@NiAl-LDHs electrodes with 3d interconnected networks architectures for high-performance pseudocapacitor storage, Adv. Mater. Interfaces 7 (2020) 2000831, https://doi.org/10.1002/ADMI.202000831.

[122] X. Wang, H. Li, H. Li, S. Lin, J. Bai, J. Dai, C. Liang, X. Zhu, Y.S. Acd, S. Dou, Heterostructures of Ni-Co-Al layered double hydroxide assembled on V4C3 MXene for high-energy hybrid supercapacitors, J. Mater. Chem. A (2019) 2291–2300, https://doi.org/10.1039/c8ta11249e.

[123] J. Zheng, X. Pan, X. Huang, D. Xiong, Y. Shang, X. Li, N. Wang, W.M. Lau, H. Y. Yang, Integrated NiCo2-LDHs@MXene/rGO aerogel: componential and structural engineering towards enhanced performance stability of hybrid supercapacitor, Chem. Eng. J. 396 (2020) 125197, https://doi.org/10.1016/J.CEJ.2020.125197.

[124] M. Chen, J. Chen, X. Tan, W. Yang, H. Zou, S. Chen, Facile self-assembly of sandwich-like MXene/graphene oxide/nickel-manganese layered double hydroxide nanocomposite for high performance supercapacitor, J Energy Storage 44 (2021) 103456, https://doi.org/10.1016/j.est.2021.103456.

[125] C. Liu, Y. Bai, W. Li, F. Yang, G. Zhang, H. Pang, In situ growth of three-dimensional mxene/metal-organic framework composites for high-performance supercapacitors, Angew. Chem. Int. Ed. Engl. (2022) e202116282, https://doi.org/10.1002/anie.202116282.

[126] L. Yue, L. Chen, X. Wang, D. Lu, W. Zhou, D. Shen, Q. Yang, S. Xiao, Y. Li, Ni/Co-MOF@aminated MXene hierarchical electrodes for high-stability supercapacitors, Chem. Eng. J. 451 (2023) 138687, https://doi.org/10.1016/j.cej.2022.138687.

[127] X. Yang, Y. Tian, S. Li, Y.P. Wu, Q. Zhang, D.S. Li, S. Zhang, Heterogeneous Ni-MOF/V2CTx –MXene hierarchically-porous nanorods for robust and high energy density hybrid supercapacitors, J Mater Chem A Mater 10 (2022) 12225–12234, https://doi.org/10.1039/D2TA02114E.

[128] M. Wang, S. Feng, C. Bai, J. Kang, J. Zhang, S. Wang, Y. Lu, D. Kong, M. Wang, S. Feng, C. Bai, K. Ji, J. Zhang, S. Wang, Y. Lu, D. Kong, Ultrastretchable mxene microsupercapacitors, Small 19 (2023) 2300386, https://doi.org/10.1002/SMLL.202300386.

[129] H. Li, X. Li, J. Liang, Y. Chen, Hydrous RuO2-decorated MXene coordinating with silver nanowire inks enabling fully printed micro-supercapacitors with extraordinary volumetric performance, Adv. Energy Mater. (2019) 1803987, https://doi.org/10.1002/aenm.201803987.

[130] S. Xu, Y. Dall'agnese, G. Wei, C. Zhang, Y. Gogotsi, W. Han, Screen-printable microscale hybrid device based on MXene and layered double hydroxide electrodes for powering force sensors, Nano Energy (2018) 479–488, https://doi.org/10.1016/j.nanoen.2018.05.064.

[131] L. Fan, W. Zheng, Y. Yang, Y. Sun, S. Peng, J. Xu, G. Yin, Bacterial cellulose composites (MXene@TOBC@PPy) for flexible supercapacitors with improved electrochemical performance, Cellulose 30 (2023) 6507–6521, https://doi.org/10.1007/S10570-023-05272-Y/TABLES/1.

[132] G. Wu, Z. Yang, Z. Zhang, B. Ji, C. Hou, Y. Li, W. Jia, Q. Zhang, H. Wang, High performance stretchable fibrous supercapacitors and flexible strain sensors based on CNTs/MXene-TPU hybrid fibers, Electrochim. Acta 395 (2021) 139141, https://doi.org/10.1016/j.electacta.2021.139141.

[133] Y. Wu, H. Hu, C. Yuan, J. Song, M. Wu, Electrons/ions dual transport channels design: concurrently tuning interlayer conductivity and space within re-stacked few-layered MXenes film electrodes for high-areal-capacitance stretchable micro-supercapacitor-arrays, Nano Energy 74 (2020) 104812, https://doi.org/10.1016/J.NANOEN.2020.104812.

[134] J. Zhang, S. Seyedin, S. Qin, Z. Wang, S. Moradi, F. Yang, P.A. Lynch, W. Yang, J. Liu, X. Wang, J.M. Razal, J. Zhang, S. Seyedin, S. Qin, Z. Wang, S. Moradi, F. Yang, P.A. Lynch, X. Wang, J.M. Razal, W. Yang, J. Liu, Highly Conductive Ti3C2Tx MXene Hybrid Fibers for Flexible and Elastic Fiber-shaped Supercapacitors, 2019, p. 1804732, https://doi.org/10.1002/smll.201804732.

[135] Y. Wu, M. Wu, D. Ho, H. Hu, Biaxial stretching array based on high-energy-efficient mxene-based al-ion micro-supercapacitor island and editable stretchablebridge, ACS Appl. Mater. Interfaces 14 (2022) 55770–55779, https://doi.org/10.1021/ACSAMI.2C17238/ASSET/IMAGES/LARGE/AM2C17238_0006.JPEG.

[136] W. Liu, C. Lu, X. Wang, R.Y. Tay, B.K. Tay, High-performance microsupercapacitors based on two-dimensional graphene/manganese dioxide/silver nanowire ternary hybrid film, ACS Nano 9 (2015) 1528–1542, https://doi.org/10.1021/NN5060442/SUPPL_FILE/NN5060442_SI_001.PDF.